A QUICK REPORT

ON

NOTO PENINSULA EARTHQUAKE ON MARCH 25, 2007

Masanori HAMADA
President

Ömer AYDAN
Chairman
Earthquake Disaster Investigation Sub-Comittee

Akio SAKAMOTO
Member, JSCE
（Tobishima Corporation, Tokyo）

April, 2007

Japan Society of Civil Engineers

1 INTRODUCTION

The Noto Peninsula (Noto-Hanto) earthquake occurred at 9:42 on JST on March 25, 2007 and it had a magnitude (Mj) of 6.9 on the magnitude scale of Japan Meteorological Agency. The earthquake killed one person and injured more than 250 people.

The strong ground motions were quite high in the epicentral area with high frequency components. The earthquake fault was associated with a known fault just off the north shore of the Noto Peninsula. This fault dips beneath Noto Peninsula. Some surface ruptures were observed in Monzen town. However, these surface ruptures might be those associated with the conjugate faults to the causative earthquake fault.

The earthquake caused the collapse of old wooden houses with heavy roofs. The highways, railways and Noto airport runway were damaged. The earthquake induced many slope failures along the steep shores and mountainous terrain

The authors investigated the earthquake affected area for three days and covered many parts of the area of concern (Figure 1.1). This report covers both scientific and engineering aspects of the earthquake. The material presented in this report is the interpretation and compilation of the available materials and information released by mass media, various earthquake-related institutes in Japan and other countries as well as the own observations of the authors and their measurements and computations.

Figure 1.1: Routes followed during the investigation (original map from MAPION)

2 GEOGRAPHY

The earthquake was located in the Noto peninsula region of Ishikawa Prefecture of Japan as shown in Figure 2.1. The area is less populated compared with other regions of Japan. The overall population of the earthquake-affected region is about 300,000. The main cities in the region are Wajima, Nanao, Suzu (Figures 2.1 and 2.2). The other large towns affected by the earthquake are Shika, Anamizu and Togi. The heavy damage was observed in the town of Monzen. Togi, which is just located nearby the epicenter, has a population of 9500.

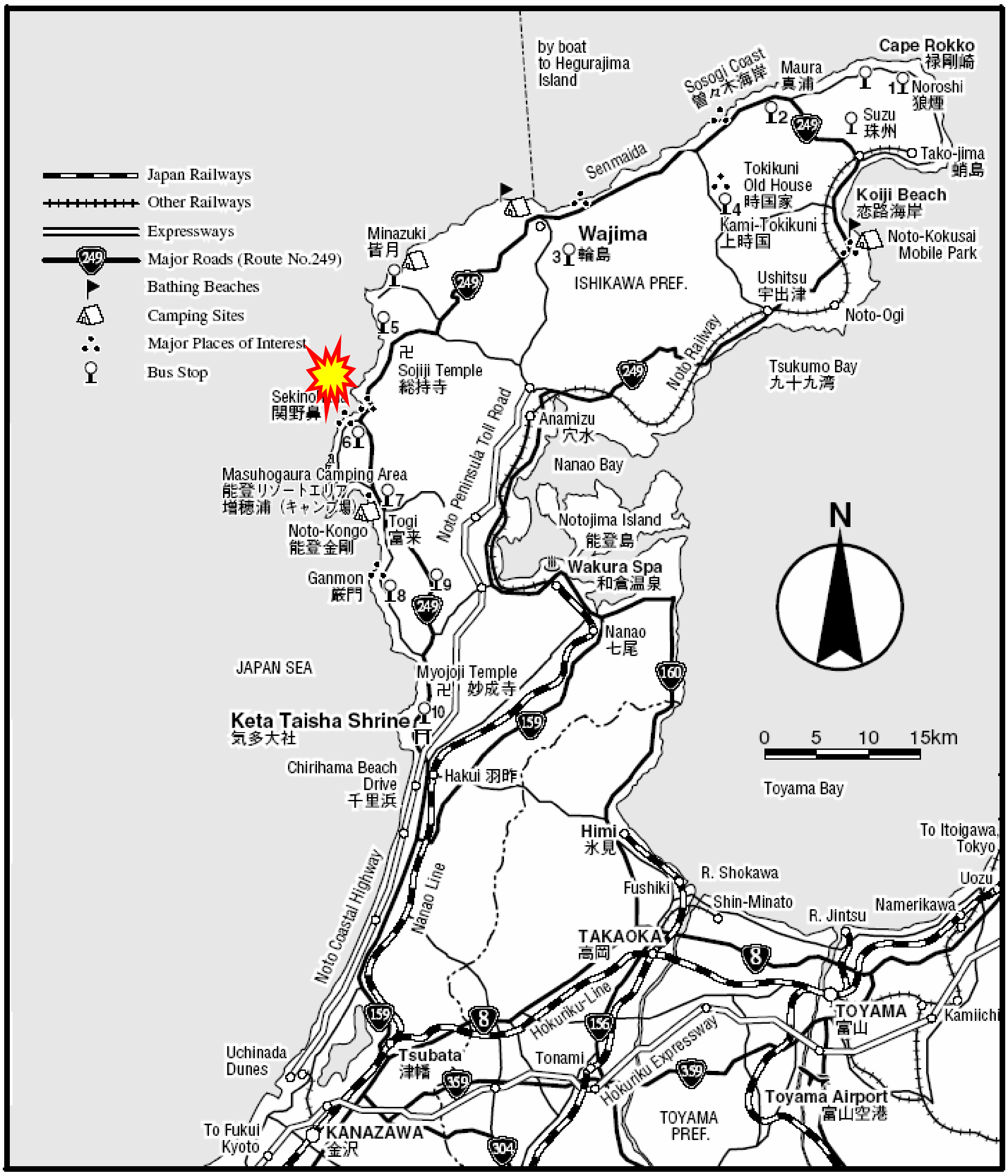

Figure 2.1 Location of cities and towns in the epicentral area (map from JNTO)

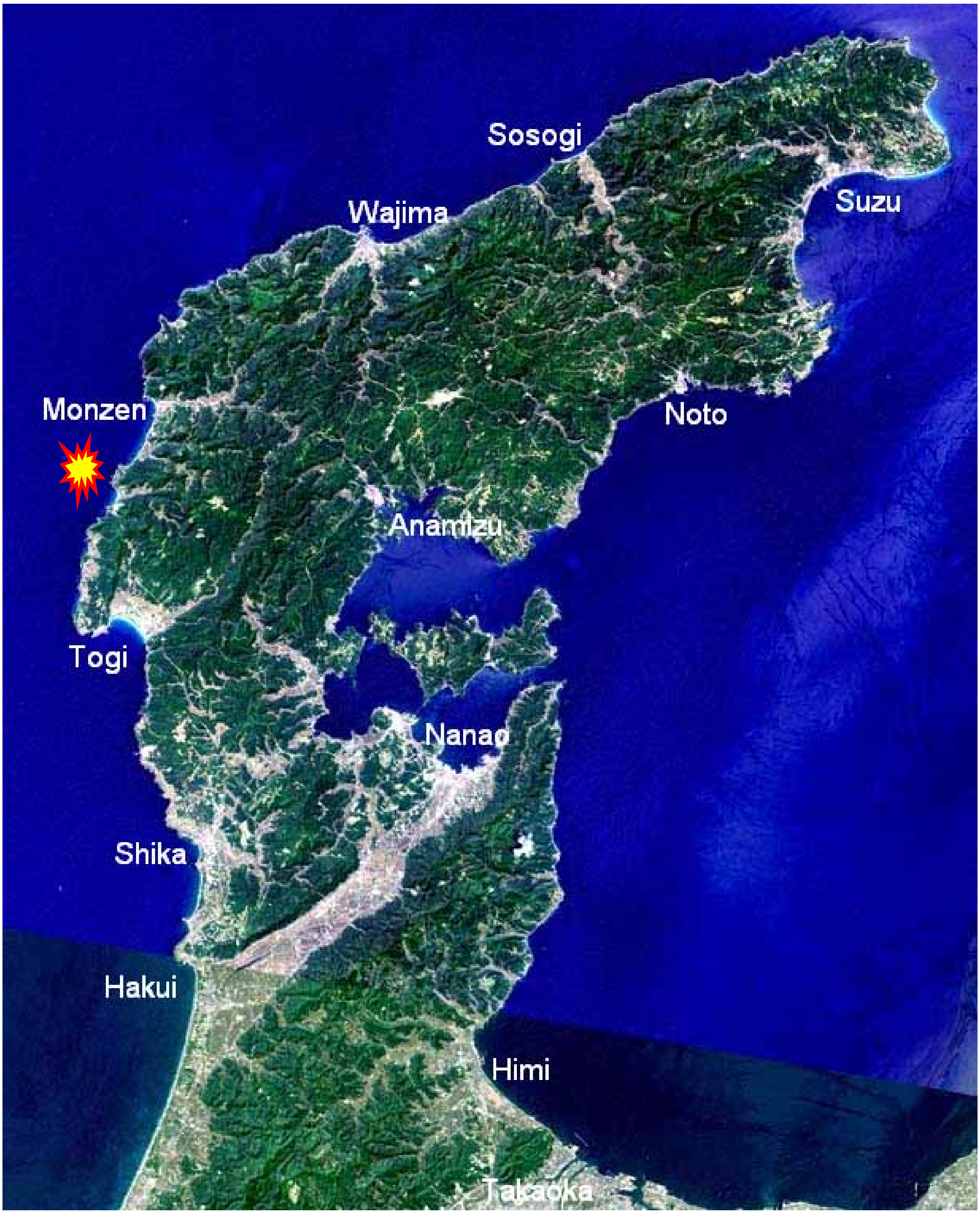

Figure 2.2: A LANDSAT view of Noto Peninsula

3 GEOLOGY AND TECTONICS

Noto peninsula mainly consists of cenozoic volcanic and sedimentary rocks overlaying Paleozoic-Mesozoic Hida gneiss and granite intrusions (Lopez and Ishiwatari, 2002) (Figure 3.1). The Cenozoic sequences composed of Oligo-Miocene volcano-sedimentary sequence. Anamizu and Yanagida formations deposited in non-marine environment. Anamizu formation includes mafic and intermediate lavas, volcanic brecia and sedimentary rocks. Yanagida formation consists of acidic pyroclastic rocks, which are mostly distributed on the northeastern part of the Noto peninsula. These volcanic formations are covered by the Miocene-Pliocene sequence composed of sedimentary and volcanic rocks formed in a marine environment.

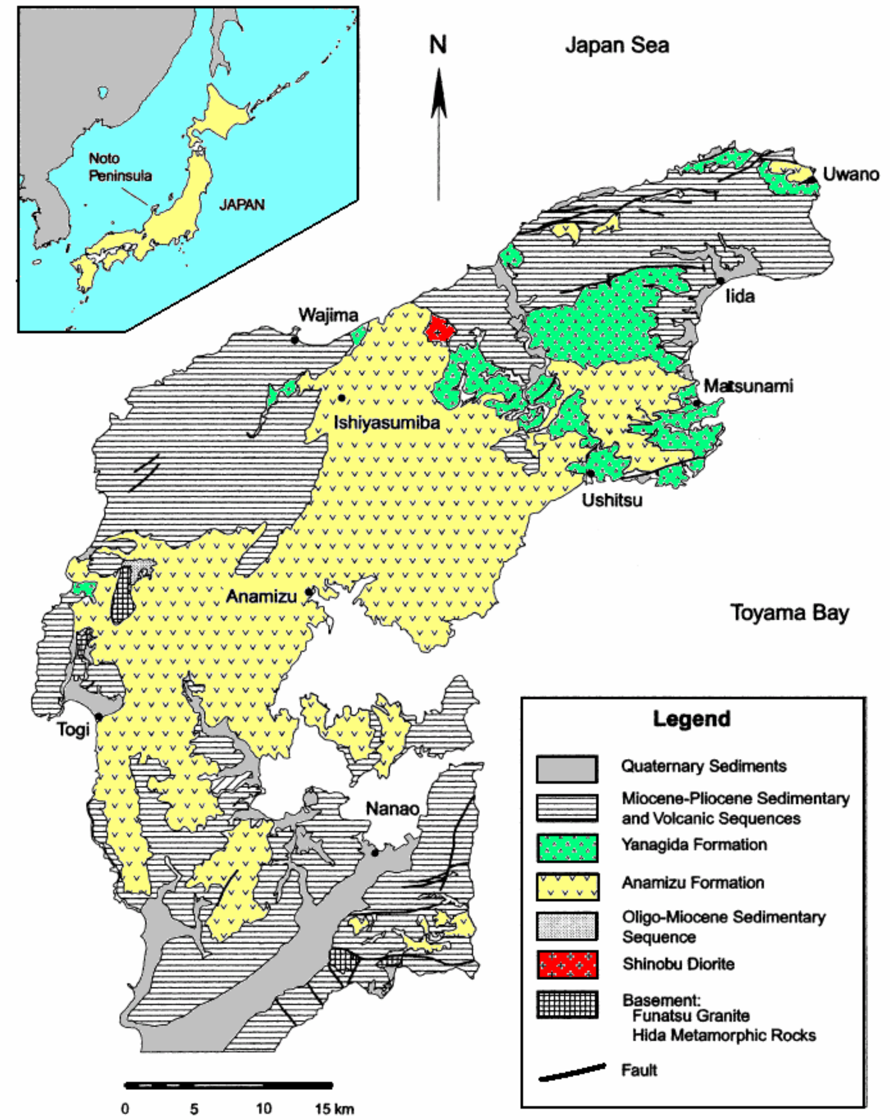

Figure 3.1: Geology of Noto Peninsula (modified from Lopez and Ishiwatari, 2002)

Anamizu formation (Notojima)

Volcanic rocks (Togi)

Volcanic rocks (Minatsuki)

Figure 3.2: Views of rock formations of Noto Peninsula

The region was disturbed by extensional deformation during the Miocene, resulting in a horst-graben structure. This period corresponds to the opening of Japan Sea. However, a subsequent compressional deformation also affected the region since Pliocene (Lopez and Ishiwatari, 2002).

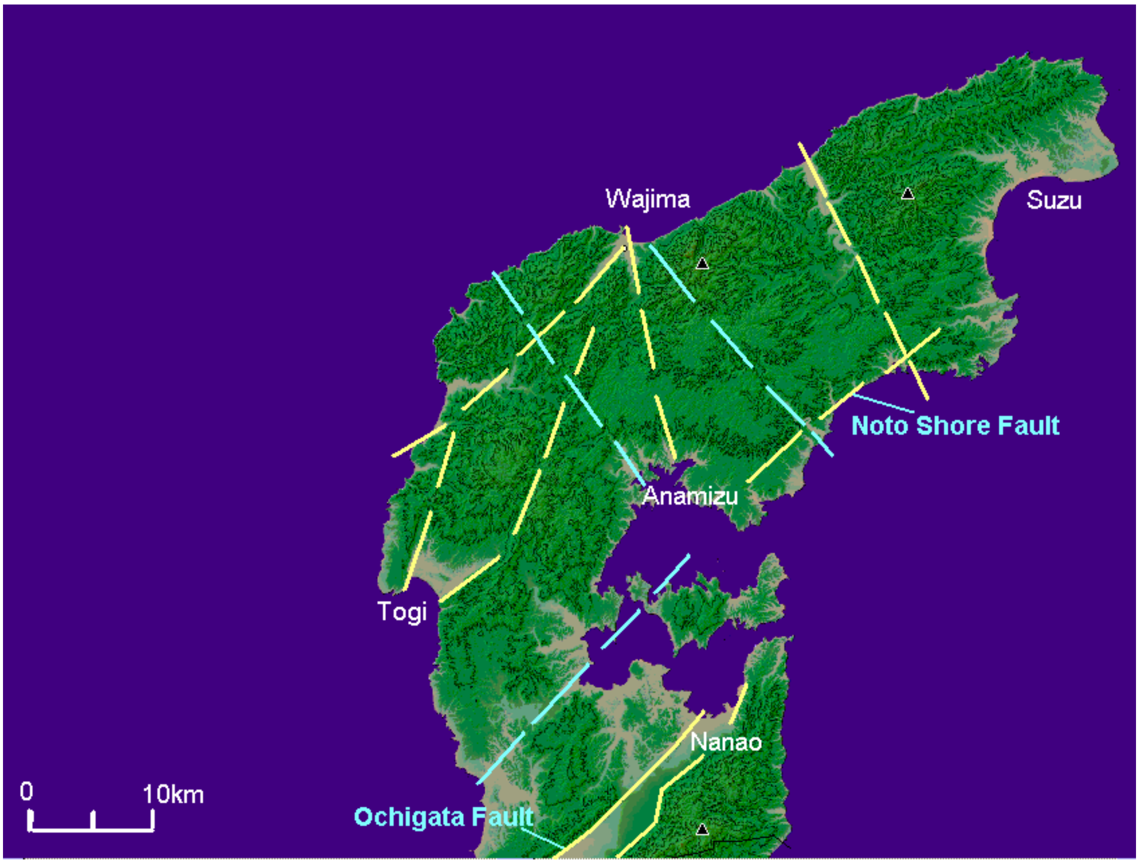

Figure 3.3: Faults and lineaments in Noto Peninsula

Japan Geology Survey (JGS) reported that Ochigata fault and Noto Shore fault are the most prominent faults with a sense of thrust faulting. The Ochigata faults are bounds to Ochigata Plain. The northern fault has a strike of N50E with an inclination of 30 to NW while the south boundary fault has a strike of N40E with an inclination of 20 to NE. The paleo-seismological trench studies on the Ochigata faults indicated that earthquakes with a net-slip of 2.2m occurred in the past. The Noto shore fault has a strike of N40E with an inclination of 60 towards NE. JGS also reported that there are thrust faults on the western side of Noto Peninsula nearby the epicentral area. The Active Fault Research Group of the JGS identified some active faults named as Isurugi thrust fault (N40E/45NW), Kanazawa thrust fault (N30E/45NE), Takashiyozu thrust fault (N30E/45NE) and Kurehayama thrust fault N40E/45NW. The authors investigated some outcrops of rock formations in the valley of Hakka and northern shore of Noto

Peninsula. Figures 3.4 and 3.5 show pictures of fault outcrops at these localities.

Figure 3.4: Thrust fault outcrop in Nakanoya district in Hakka valley

Figure 3.5: Normal fault outcrop nearby Ozawa at Northern shore of Noto Peninsula

4 SEISMICITY

4.1 Past Seismicity

The past seismological records indicate that the region experiences some large events from time to time. Most of the events are of intra-plate type. Figure 4.1 shows locations of past seismic events as well as recent events with known focal plane solutions. The focal plane solutions indicate that the dominant faulting mechanism of seismic events is thrust type faulting in/around Noto Peninsula. The most recent event occurred on February 7, 1993. The faulting mechanisms of the 1933 and 1993 events were quite similar to that of the 2007 event. The seismicity shown in Figure 4.2 is aligned in certain directions, which generally correspond to known fault traces in/around Noto Peninsula.

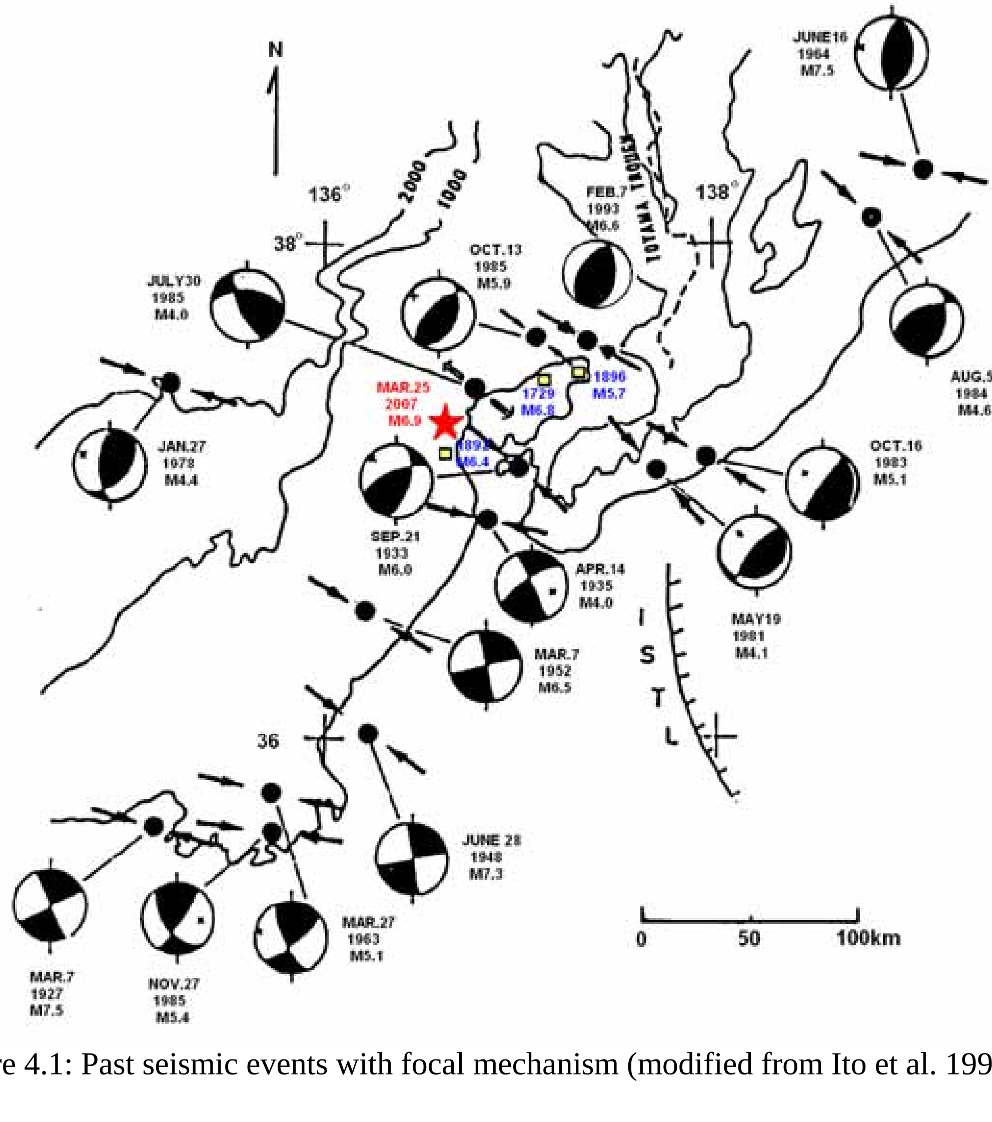

Figure 4.1: Past seismic events with focal mechanism (modified from Ito et al. 1994)

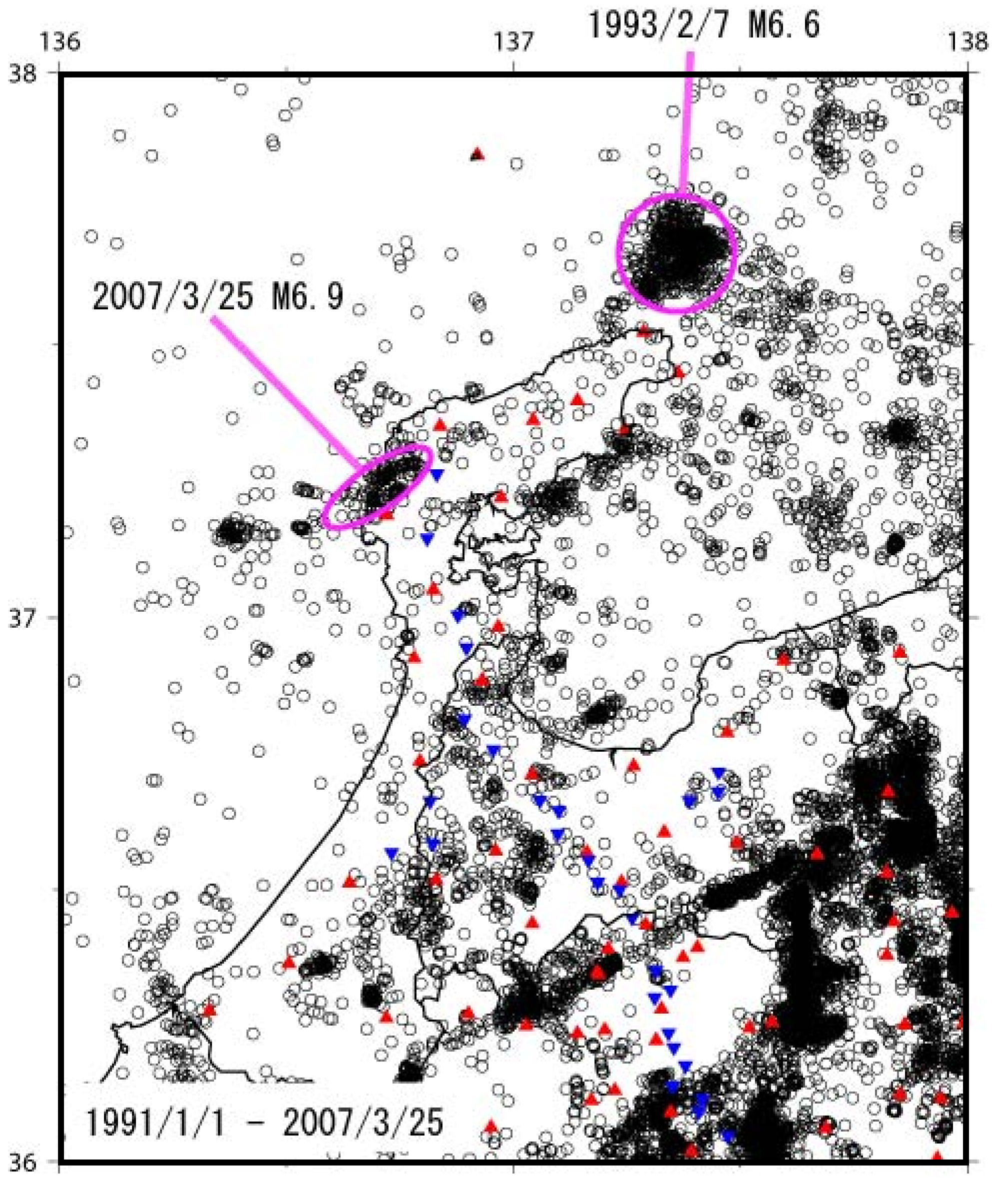

Figure 4.2: Seismicity between 1991/1/1 and 2007/3/25 (from ERI, 2007)

4.2 Epicenter Estimations

Different seismological institutes estimated the epicenter locations as shown in Figure 4.3. While the epicenters estimated by USGS and HARVARD are very close to each other, the epicenters by JMA and NIED are somewhat different and they are close to shoreline. However, the epicenter estimated by the Hi-NET of Japan is very close to those by USGS and HARVARD. The difference probably associated with the velocity structure adopted during the inverse analysis.

Figure 4.3: Locations of epicenters estimated by different seismological institutes

4.3 Post Seismicity and Aftershock Distributions

Since the epicenter data of aftershocks determined by Japan Meteorological Agency (JMA) are available on INTERNET, the data released by the JMA is used to infer the possible dimensions of the activated fault plane. Figure 4.4 shows the epicenter distributions together with cross-sectional and longitudinal distributions of aftershocks in selected directions. There are two large aftershocks located at both ends of the presumed fault. The distributions of aftershocks on March 25 indicate that the main fault should be about 25-30km long and 10-15km wide. However, a 40km long zone is activated during the re-adjustment of disturbed crustal stresses by the earthquake.

The projections of aftershocks on the cross-sections indicated in Figure 4.4 imply that the fault inclination should be ranging between 45-50. This inclinations is close to that obtained by HARVARD described in next section.

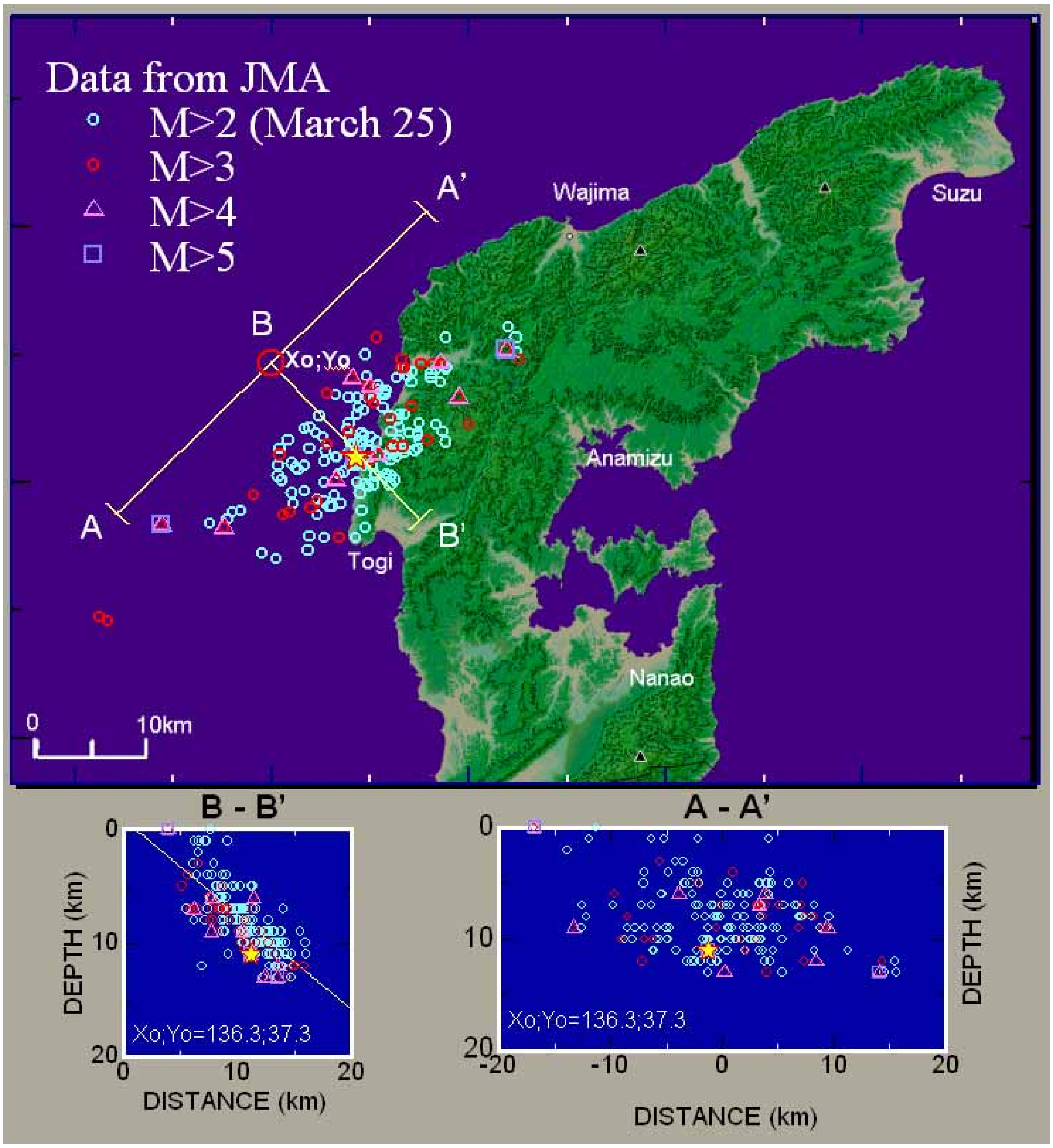

Figure 4.4: Post-seismicity and aftershock distributions (data from JMA)

5 CHARACTERISTICS OF THE EARTHQUAKE AND FAULTING

The parameters of focal plane solutions estimated by different seismological institutes in Japan and worldwide are listed in Table 5.1 and illustrated in Figure 5.1. The fundamental mode of faulting was thrust-type with a slight dextral component. Many institutes estimated that the fault dipping SE would be the causative fault from the computed mechanisms. Except the solution of the HARVARD, most of institutes estimated that the dip of the causative fault should be quite steep. However, the after-shock activity indicated that the inclination of the fault would be quite similar to that estimated by HARVARD. The fault plane is estimated to be about 22-40km long and 14-25km wide.

Table 5.1: Parameters of the earthquake estimated by different institutes

Institute	Latitude	Longitude	Depth (km)	Magnitude	Strike	Dip	Rake Angle
JMA	37.220	136.685	11	Mj=6.9	NP1 318^o NP2	29^o	107^o
HARVARD	37.280	136.600	12	Mw=6.7	NP1 46^o NP2 182^o	45^o 55^o	124^o 61^o
USGS	37.537	136.438	7	Mw=6.6	NP1 58^o NP2 193^o	60^o 40^o	117^o 52^o
NIED	37.200	136.700	8	Mw=6.7	NP1 58 NP2 173	66 48	132 34
ERI			4	Mw=6.7	NP1 60^o NP2	72^o	120^o
TU-Yagi	37.286	136.652	8	Mw=6.7	NP1 47^o NP2 121^o	51^o 61^o	116^o 79^o

The rupture parameters of the earthquake estimated by different seismological institutes are given in Table 5.2. Figure 5.2 shows the estimated slip distribution by JMA using Kikuchi-Aki’s method. The estimated maximum slip is in the order of 1.6m and it is expected to appear in the sea and the rupture front would follow a line parallel to the northern shore of Noto Peninsula. In other words, the expected rupture front should appear in the sea along the northern shore of Noto Peninsula. The ruptures, which may appear on the ground, would be related to secondary events associated with the causative fault. Considering the extensive rock slope failures in 2005 Kashmir earthquake and model tests on thrust faulting, the deformation front may be diluted by extensive rock slope failures. The authors plotted the locations of rock slope failures, liquefaction locations and observed surface ruptures in Figure 5.3 and views of surface ruptures observed by the authors (Figure 5.4).

Table 5.2: Parameters of the earthquake estimated by different institutes

Institute	Length (km)	Width (km)	Duration (s)	Slip (mm)	Rupture Velocity (m/s)	Rise Time(s)
JMA	35.00	22.00	11	1600		
HARVARD			10.6			
GSI	21.20	13.90		1650		
NIED	36.00	24.00		3000	3.4	
ERI	33.33	16.66	10	3000		
TU-Yagi	40.00	15.00	14	1600	2.5	
JGS-AFG	25.00	20.00			3.0	

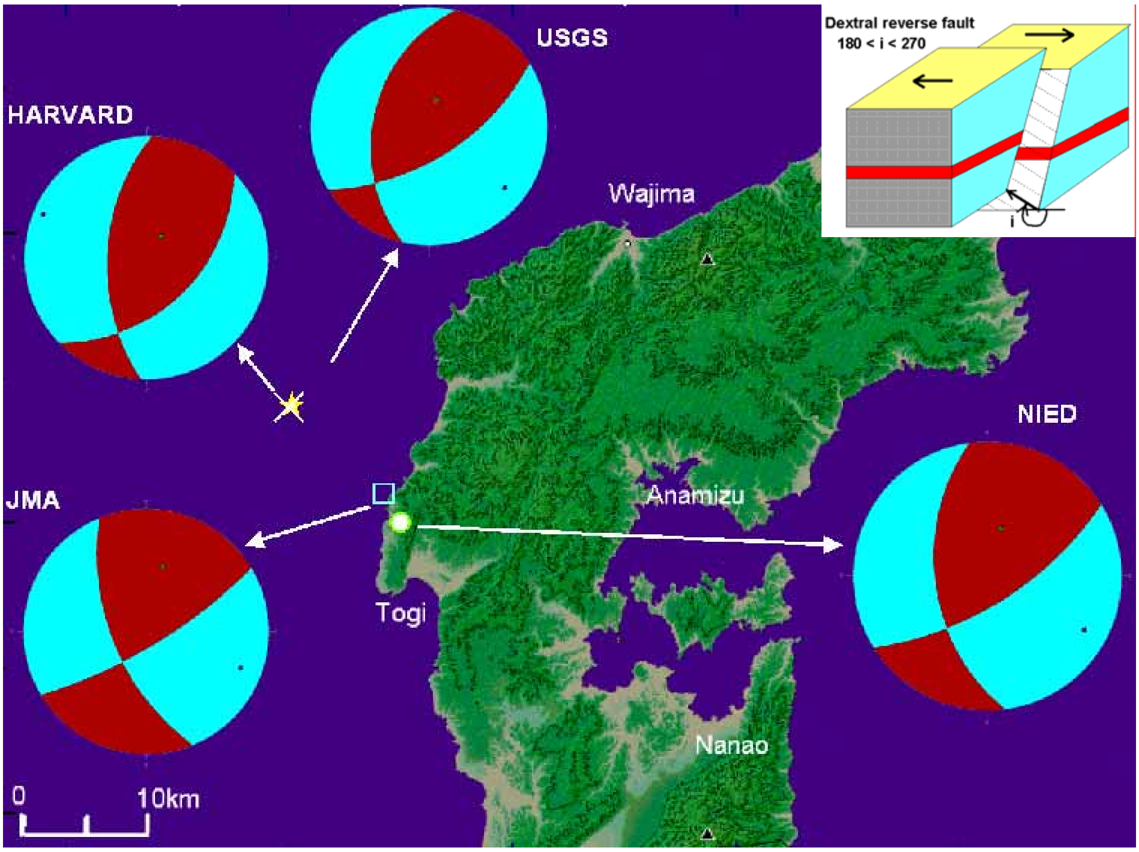

Figure 5.1: Focal plane solutions by different seismological institutes with a physical interpretation

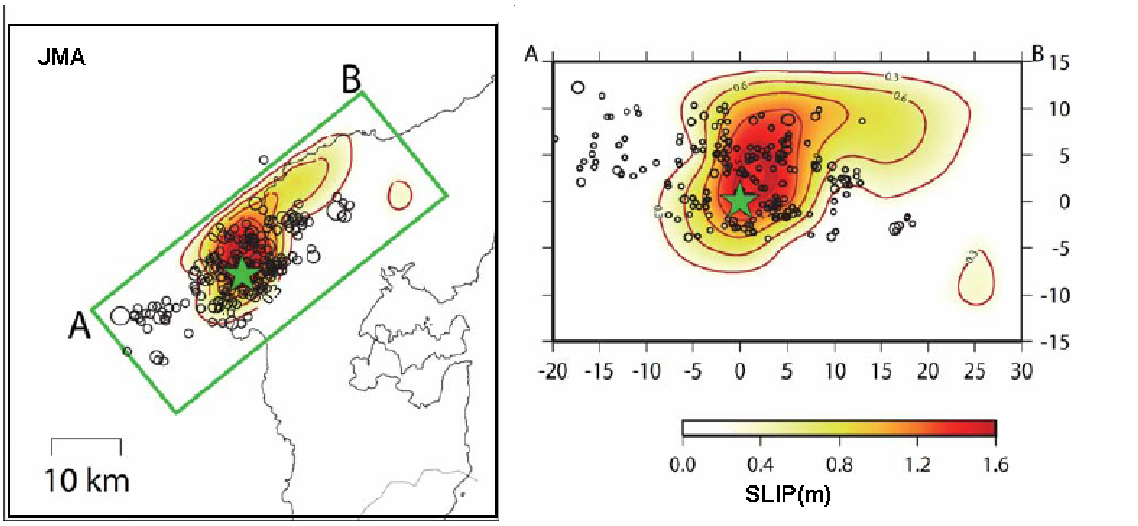

Figure 5.2: Estimated slip propagation by JMA

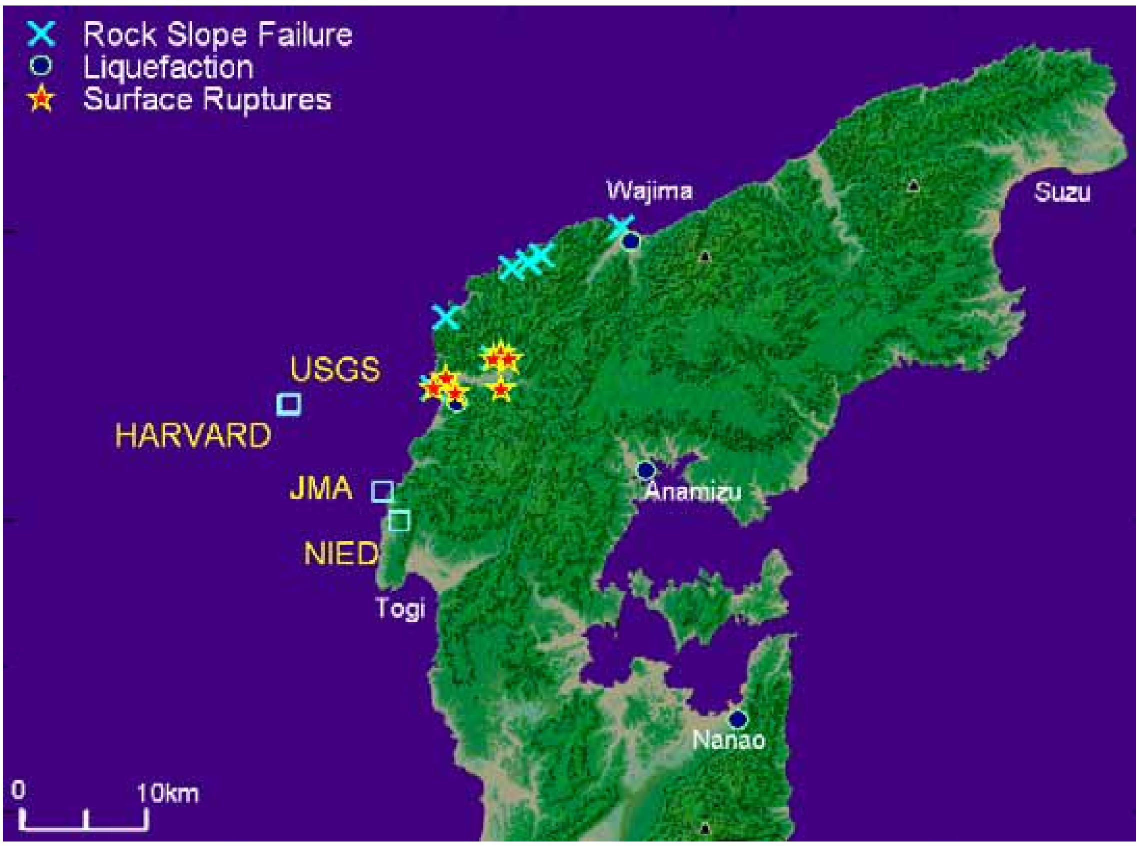

Figure 5.3: Locations of surface ruptures, large rock slope failures and ground liquefaction

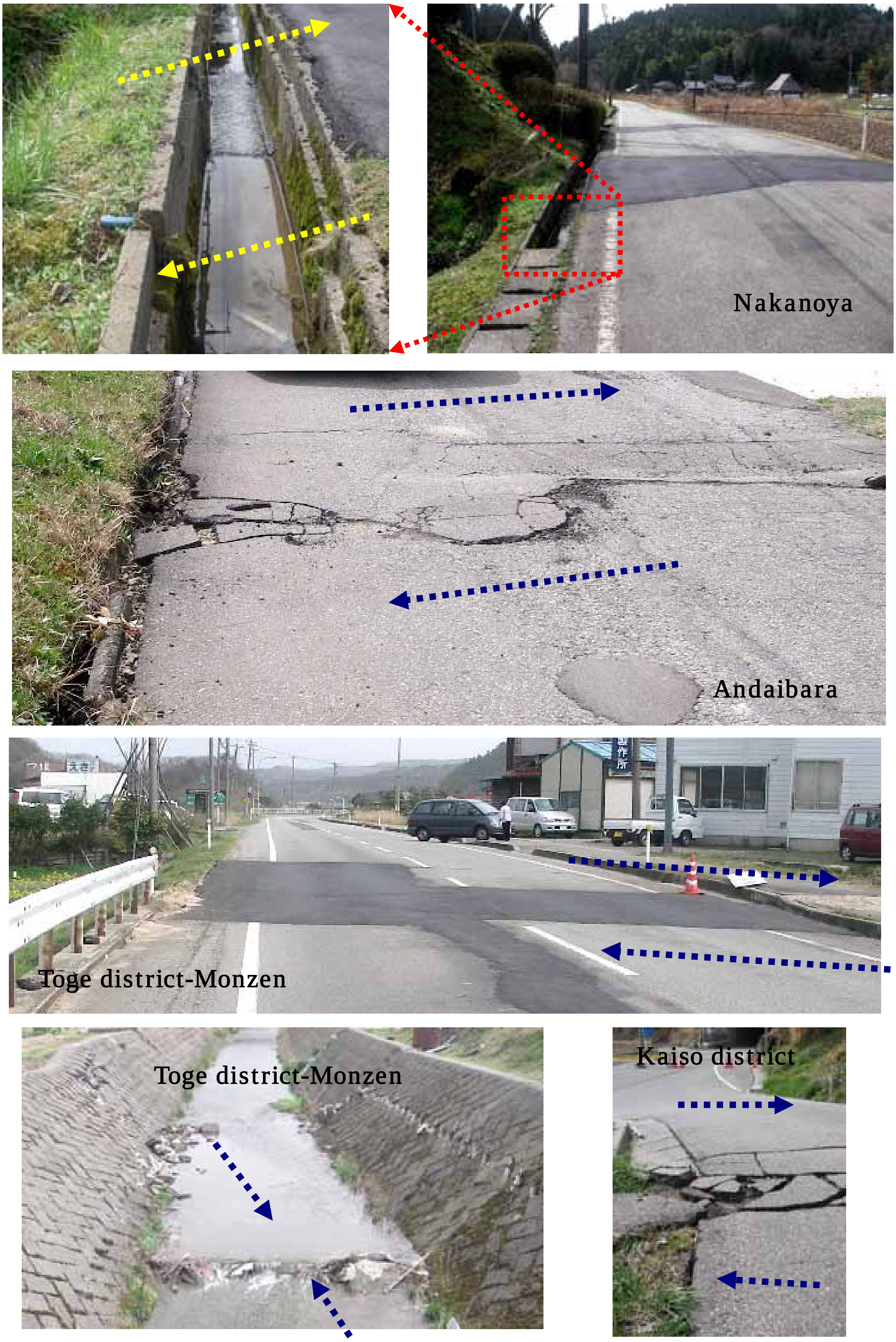

Figure 5.4: Close up views of locations of observed surface ruptures

The authors also noted some vertical movements of seashores at three localities, namely, Kaiso, Ozawa and Wajima shores (Figure 5.5). Although it may be difficult to differentiate the effects of tides on the shore line, it seems that the vertical ground movements would be more than 500mm at the seashore nearby Kaiso ports while it would be about 200-250 mm at Wajima Tide Gauge Station.

Figure 5.5 Possible uplifts nearby Kaiso, Ozawa and Wajima ports

6 STRONG GROUND MOTIONS

The strong motion networks of Japan Meteorological Agency and K-Net and Kik-Net of NIED recorded very high ground accelerations in the epicentral area. The maximum ground acceleration was observed in Togi, which was the nearest strong motion station to the epicenter, and it was more than 850 gal while the ground acceleration was 782 gal in Anamizu.

Figure 6.1 shows the acceleration records at several locations around the epicenter. As noted from the acceleration records, they are strikingly different from each other.Togi is on the hanging-wall of the causative fault. On the other hand, Wajima is at the east-end of the causative fault and it has a more impulsive character. These records clearly indicate the characteristics of ground acceleration differ from each other and there is a strong directivity effect associated with rupturing process as noted from Figure 6.2. Figure 6.3 is a comparison of attenuation of maximum ground acceleration with empirical relations. The observed results indicate that the amplification of accelerations may be 4 to 5 times that on the hard ground. The damage observed in the epicentral area clearly confirm this conclusion. The contours of maximum ground velocity and its attenuation are plotted in Figures 6.4 and 6.5. Although the general characteristics are same, the unusual maximum ground velocity at Anamizu station is probably due to peculiar ground conditions and contours are biased by the data of the Anamizu station.

Figures 6.6 to 6.8 show acceleration response spectra for Togi, Wajima, Noto and Anamizu records with a damping ratio of 5%. Togi and Wajima response spectra have some similarities while their absolute values are different. While the peak acceleration spectra values are almost same for Togi and Anamizu for EW component, the periods at the peak accelerations are different from each other. In other words, the structures having shorter period should be more affected in Togi and Wajima while structures with longer periods would be affected by the shaking in Anamizu. Nevertheless, the response acceleration values can be 4-5 times the base acceleration. The geological conditions for Anamizu strong motion station is shown in Figure 6.9

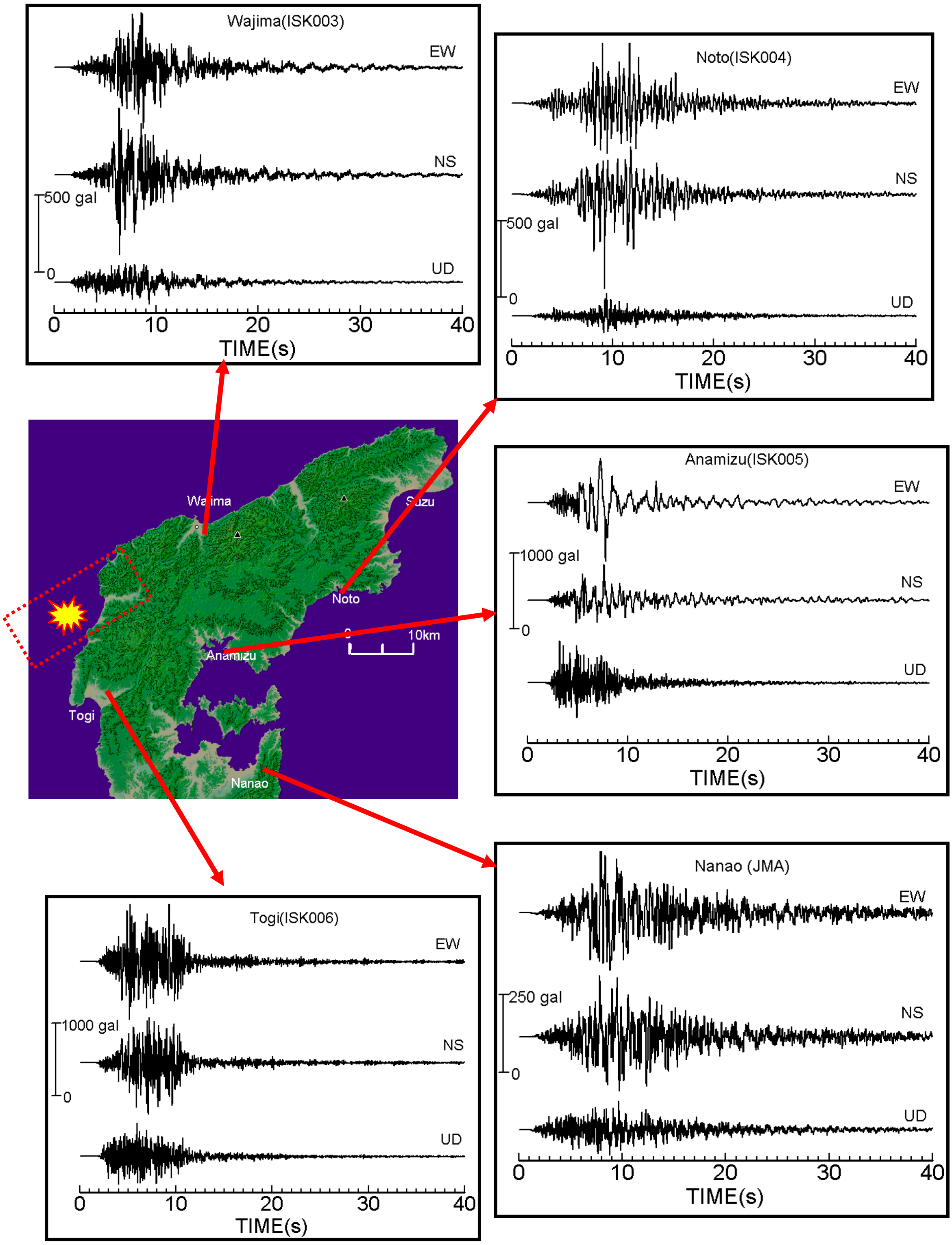

Figure 6.1: Acceleration records in the vicinity of the earthquake epicenter

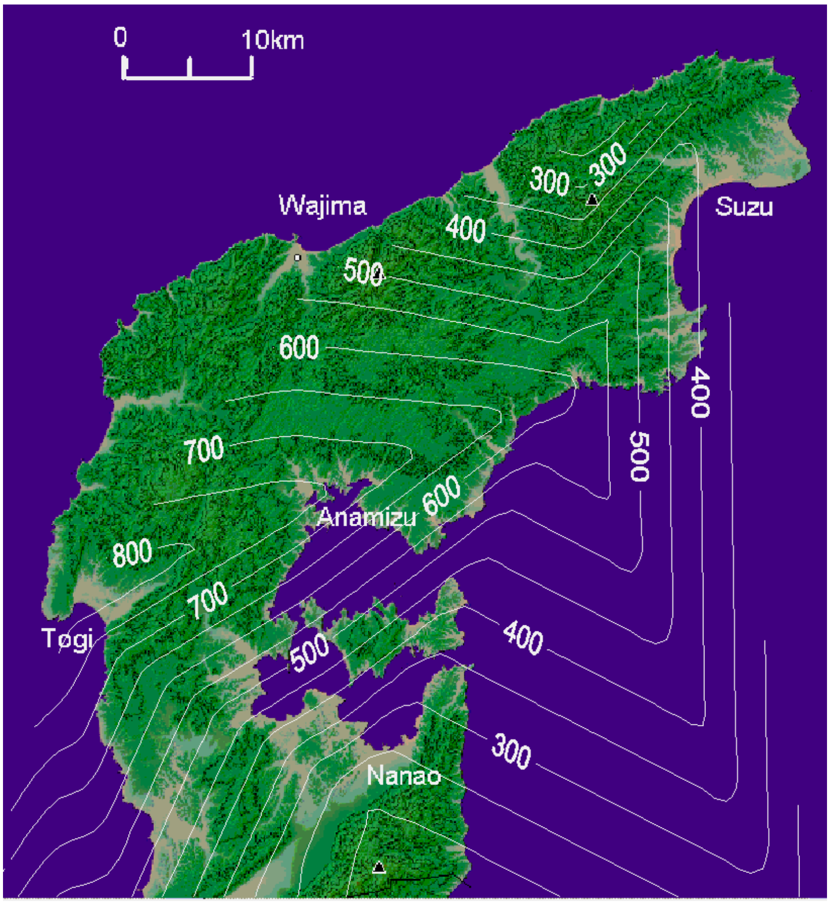

Figure 6.2: Contours of maximum ground acceleration (Amax)

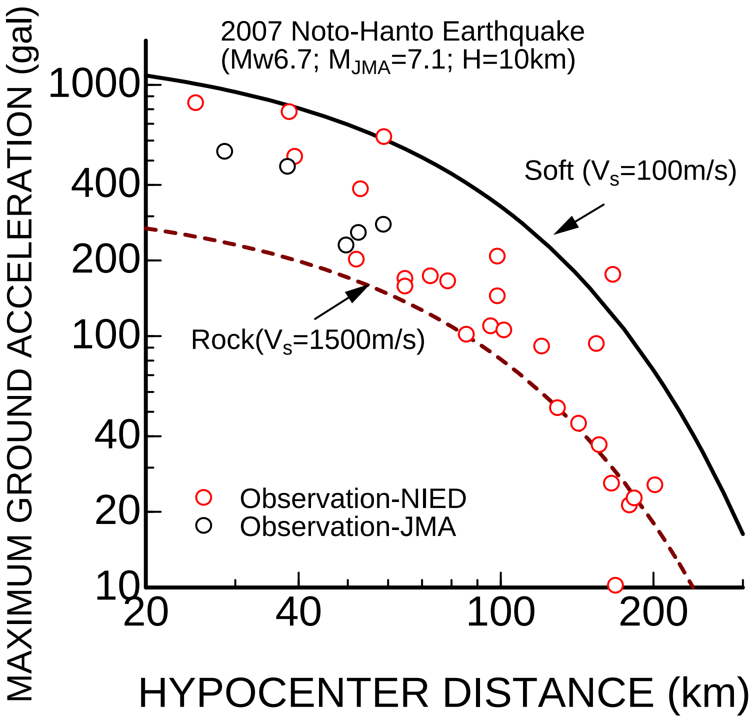

Figure 6.3: Attenuation of maximum ground acceleration (Amax)

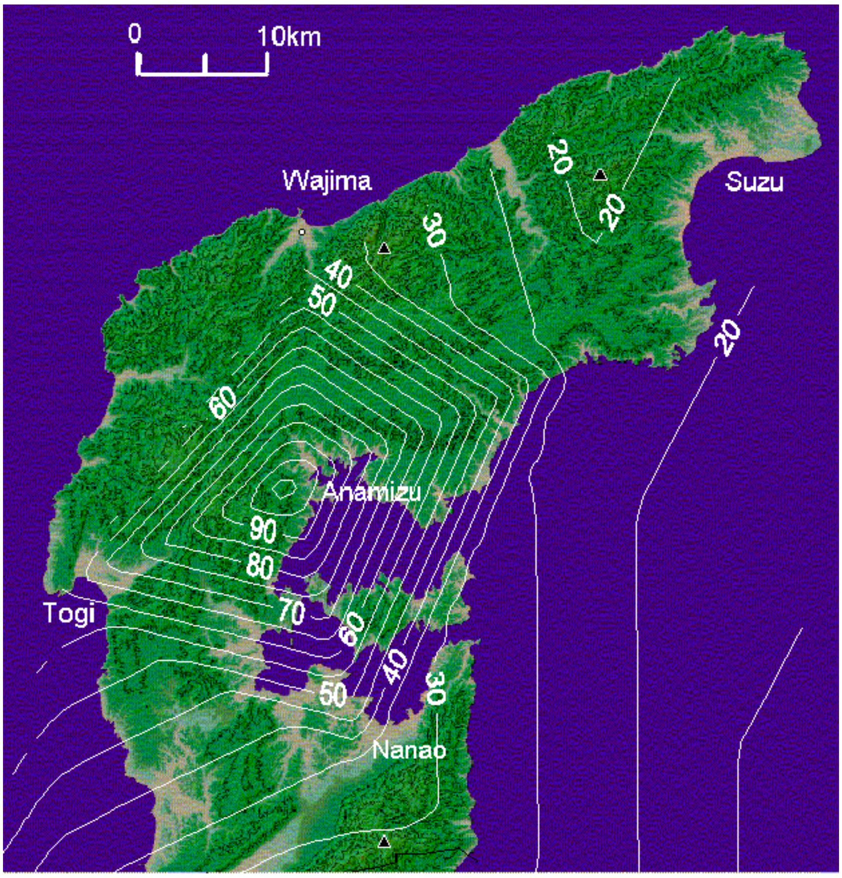

Figure 6.4: Contours of maximum ground velocity (Vmax)

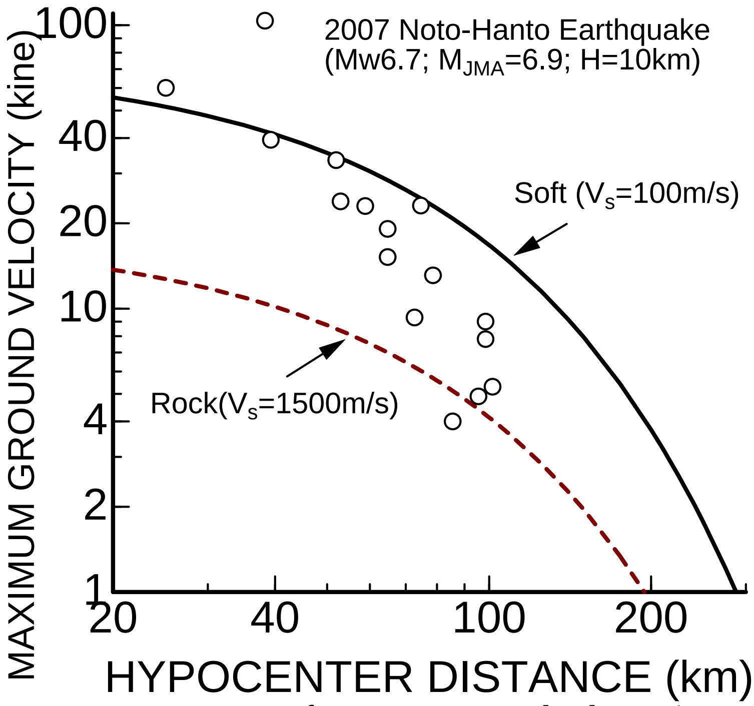

Figure 6.5: Attenuation of maximum ground velocity (Vmax)

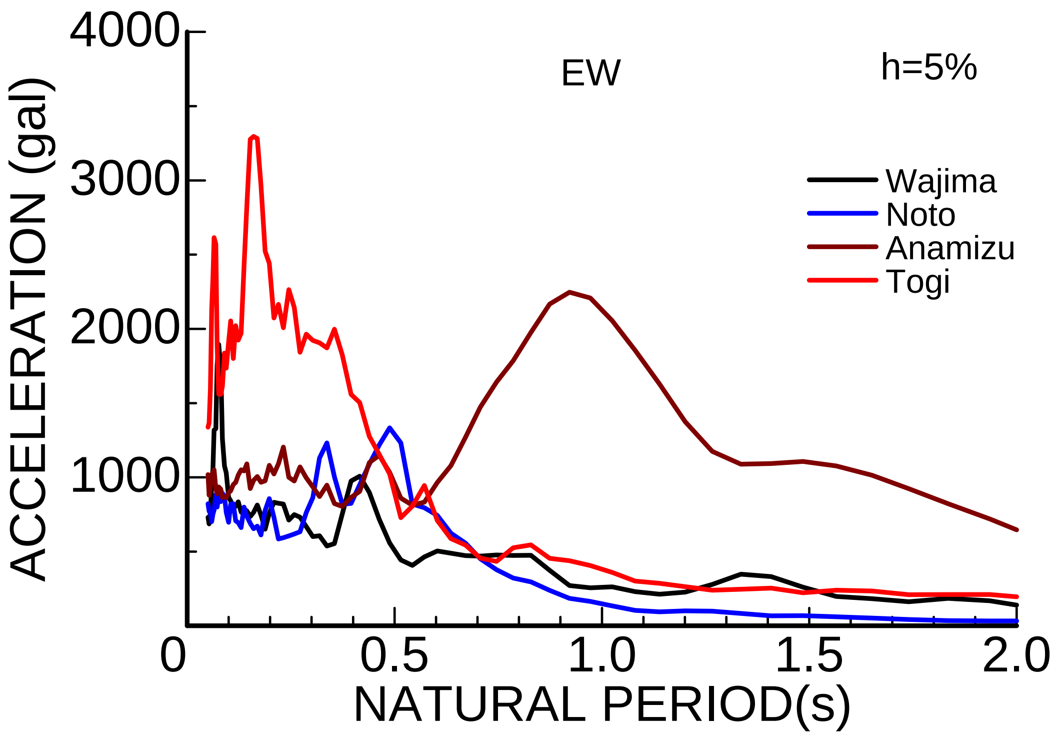

Figure 6.6 Acceleration response spectra for EW component

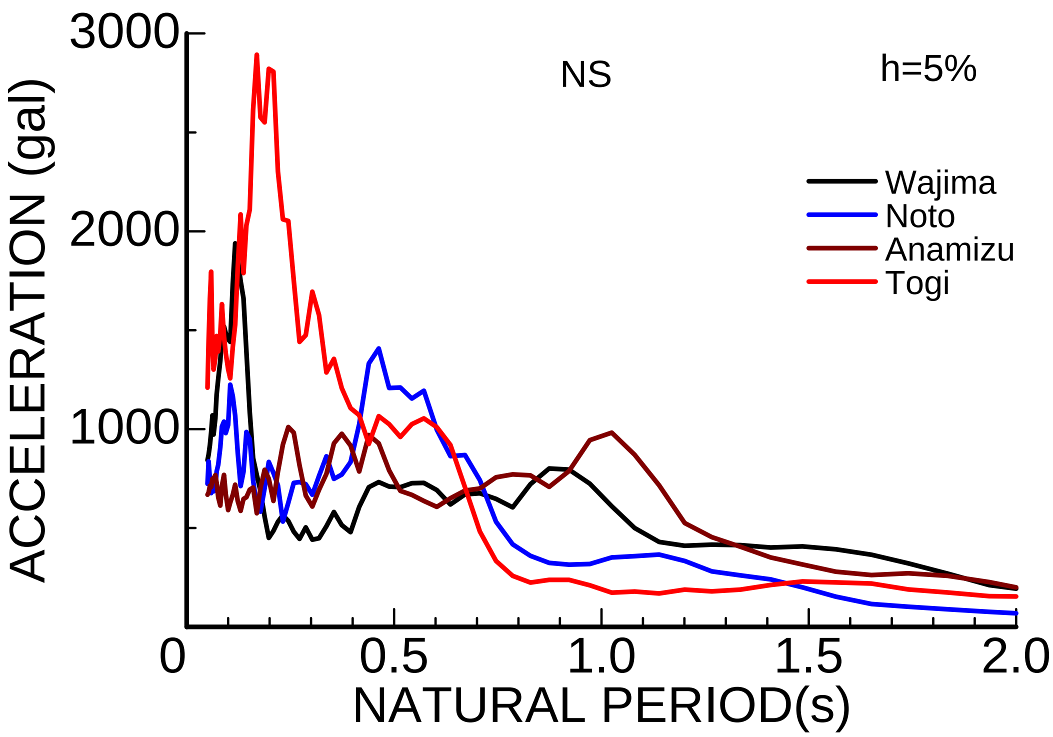

Figure 6.7 Acceleration response spectra for NS component

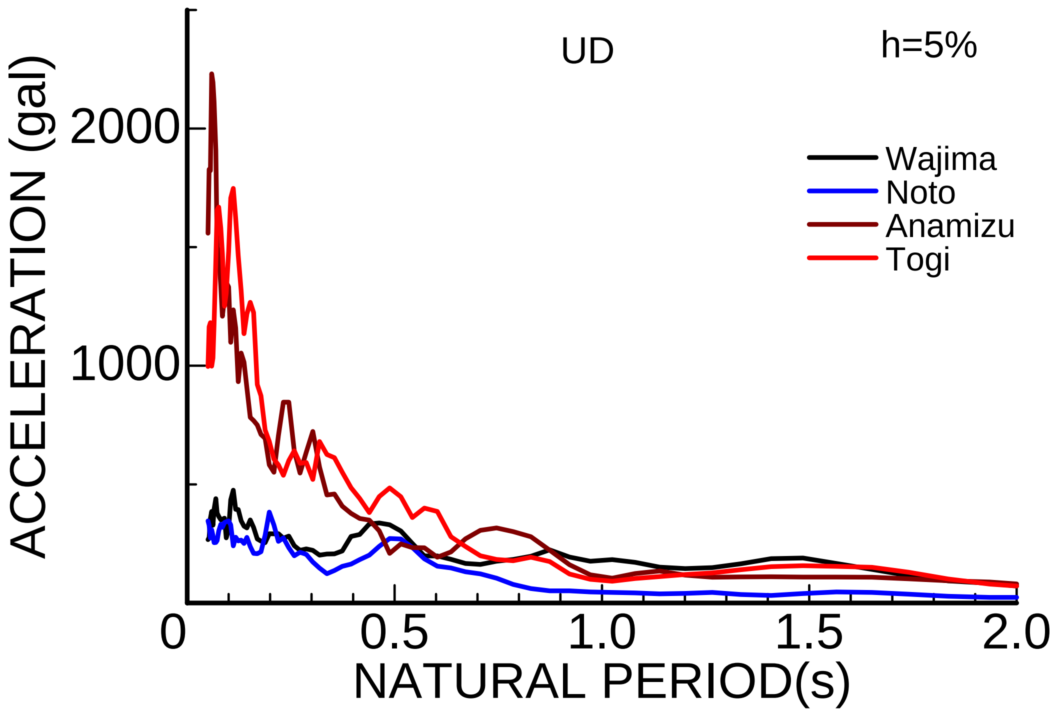

Figure 6.8 Acceleration response spectra for UD component

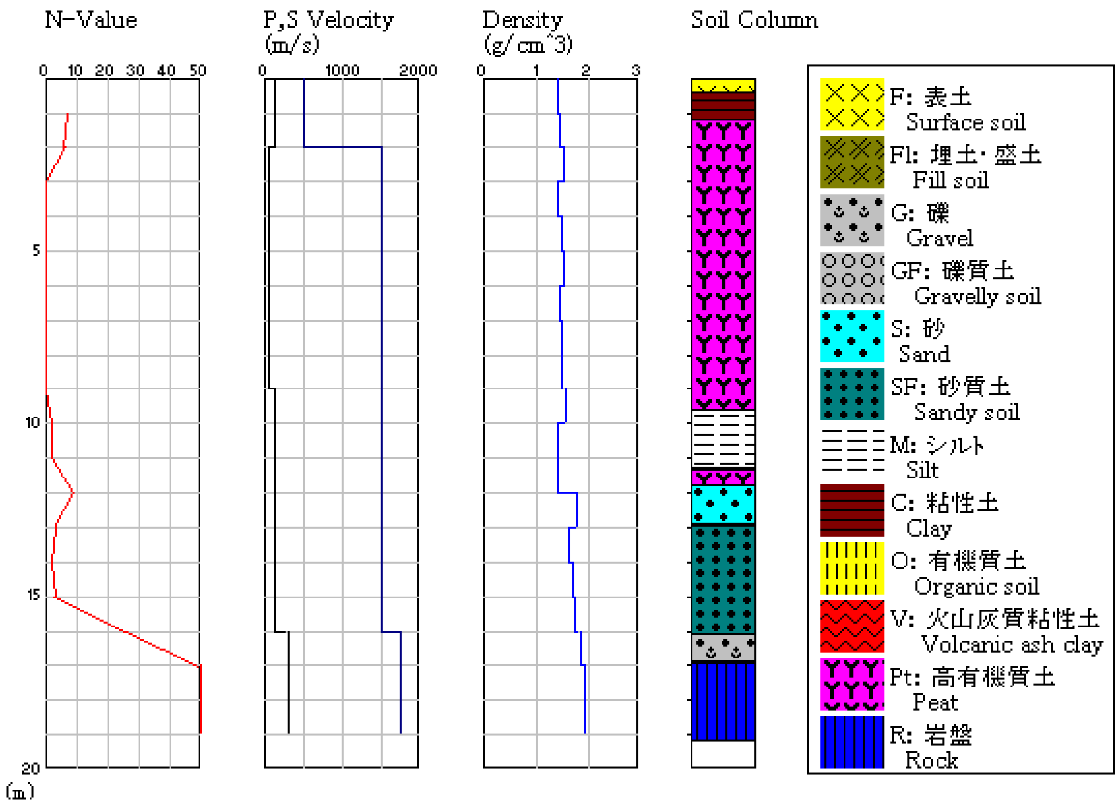

Figure 6.9: Geological conditions at Anamizu strong motion station (K-NET)

7 DAMAGE TO STRUCTURES

7.1 Building Damage

7.1.1 Wooden houses

Mainly old wooden houses either collapsed or were heavily damaged. The failure was quite similar to those observed in 1995 Kobe earthquake. The failure mechanism fundamentally involved hinging of wooden columns at the base and also at the connections between 1st floor and 2nd floor as a result of large horizontal earthquake forces (Figure 7.1). The traces of such mechanism can be seen widespread in the epicentral area. In addition some relatively new wooden houses either collapsed or were damaged. The main cause was the weak floor situation observed at the first floor used as garage, workshop or storage. Some houses either collapsed or were damaged due to slope or embankment failure, on which they were built (Figure 7.2). This type of failure observed in mainly hilly regions and also nearby creeks and rivers. The heavy damage at Toge district of Monzen town was partly surface ruptures associated with faulting and lateral spreading of loose sand ground. The authors found boiled sand volcanoes at several locations in this district (see chapter 8).

Figure 7.1: Some typical examples of collapsed or heavily damaged wooden houses

Figure 7.2: An example of damaged house built on an embankment in Monzen town

7.1.2 RC Buildings

RC buildings in the epicentral region are few and they are used as schools, public offices and a few as residential buildings. The number of stories is mostly 3 to 5. Furthermore, the infill walls of the RC buildings are reinforced concrete shear-walls. Some of public reinforced buildings were retrofitted with steel frame bracing. Almost all reinforced concrete buildings performed well during the earthquake. The observations and investigations in many cities and towns indicated that RC buildings were generally none or slightly damaged in spite of high ground accelerations. The shear-walls of the RC building of NTT in Wajima city experienced some cracking as seen in Figure 7.3. However, it should be noted that the damaged section of the building supports a high transmission tower on its roof.

7.1.3 Temples

Damage to temples was generally observed at fort-gate (torii) made of granitic columns and beams. One spectacular example was observed at Soji Temple next to the NTT building. The granitic column were uprooted from their base and toppled as seen in Figure 7.3(a). The main compounds were generally non-damaged (Figure 7.3(b)) due to superior earthquake-resistant-ability.

Figure 7.2: Non-damaged reinforced concrete building in Monzen town

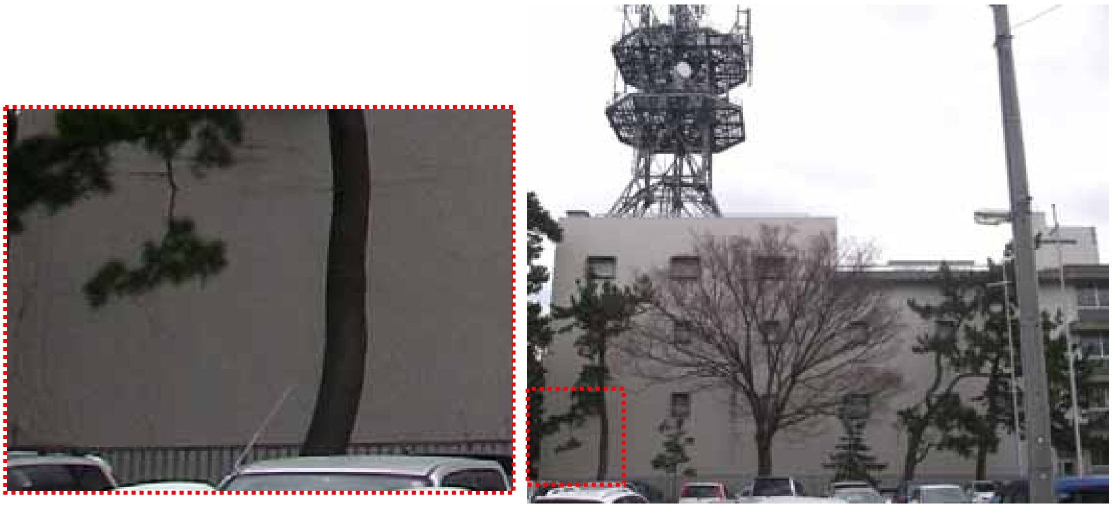

Figure 7.3: NTT building and close-up view of cracked shear walls

(a) Toppled fort-gate of Soji temple

(b) Intact compound of Sojiji Temple

Figure 7.4: Some views of damaged and non-damaged temples

7.2 Damage to Transportation Facilities

Most of land transportation in Noto Peninsula is done through state and prefecture roadways and Noto Toll way (Figure 7.5). The railway network is not dense and most of railways lines were abandoned due to financial problems. The air transport is available between Tokyo and Noto Airport. The sea transportation is mostly for shipping and fishing. In this subsection, the effects of the earthquake on transportation facilities are described.

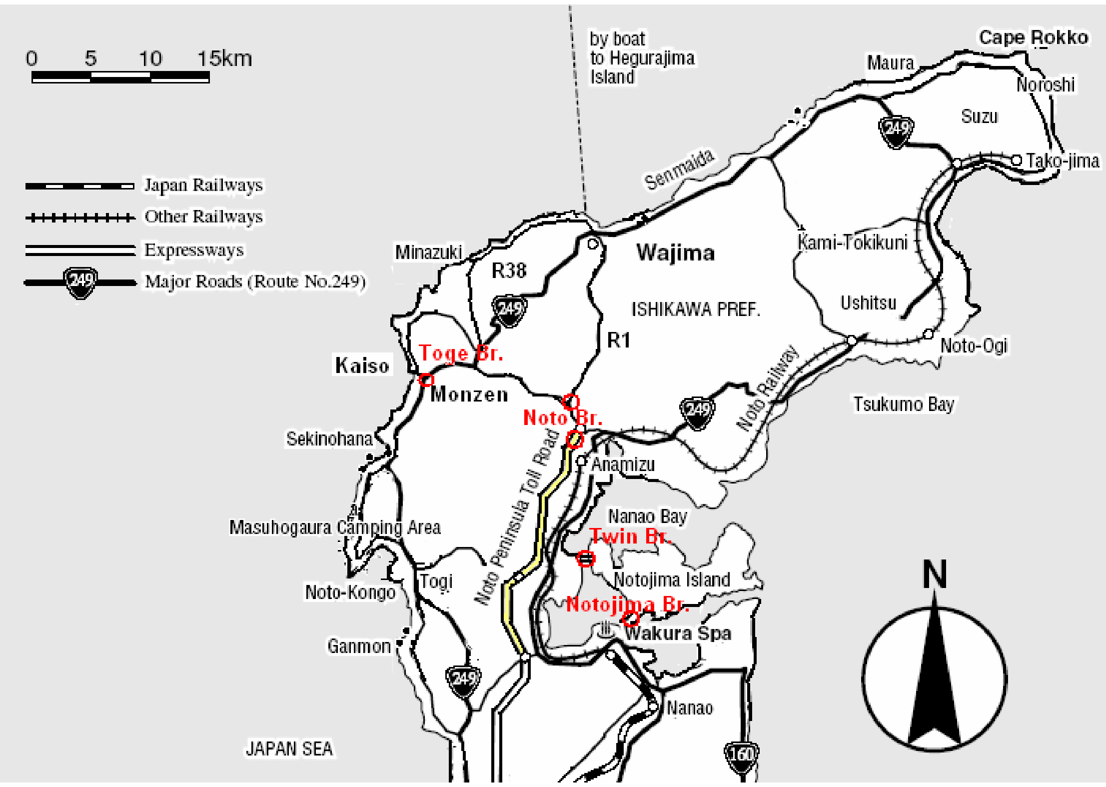

Figure 7.5: Roadway and railway network of Noto Peninsula

7.2.1 Railways

The railway network of Noto Peninsula is not dense as compared with other parts of Japan. Japan Railways extends up to Nanao city and the Noto railway line operated by the third sector runs between Nanao and Anamizu. The line between Anamizu and Suzu is not in operation any longer. The effect of the earthquake was quite negligible on JR lines. Nevertheless, trains were stopped until the safety of the railways checked. JR lines were back to operation on March 26, 2007. The railway line between Anamizu and Nanao were damaged at 25 locations due to deformation of rails. Some repairs of rails on the line between Anamizu and Nanao were carried out soon after the earthquake and the railway line was in operation on March 30, 2007 after 5 days. Buses were used as a temporary measure to deal with train stoppage.

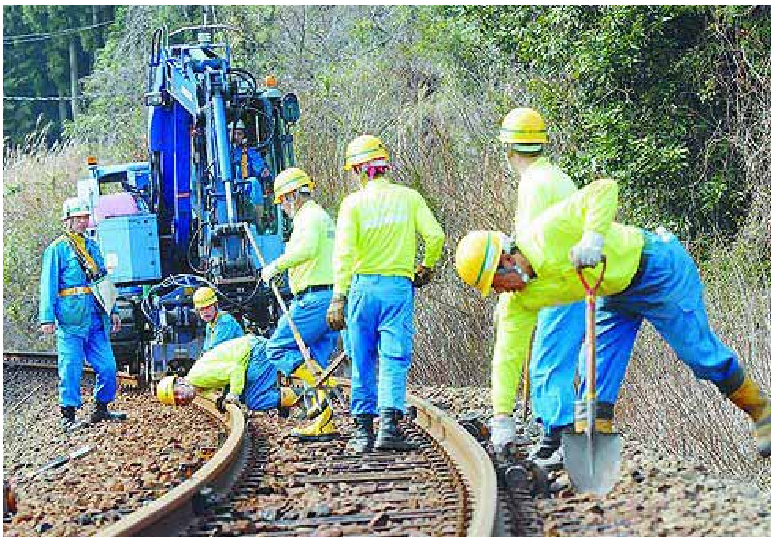

Figure 7.5: A repair work on Anamizu-Nanao railway line (from Yomiuri Newspaper)

7.2.2 Roads, Highways, Expressways

Surface ruptures and settlement of ground damaged roads in Monzen town (Figure 5.4). Furthermore, they were either obstructed or damaged by slope failures and rock falls. The settlement of embankments of roadways at bridges were generally more than 100-200mm. The settlement was caused by either ground shaking or ground liquefaction at some places. In addition, the settlement of improperly compacted infill material of sewage lines was extensively observed and the settlement was particularly amplified at manholes.

Figure 7.6: Some examples of damage to roadways

Highways R1, R249, R38 pass through the epicentral region. These highways built on existing ground or embankments were damaged in various parts due to either the failure and/or settlement of embankments and slope failure (Figure 7.7). The 249 Highway was obstructed by slope failures at Maura. R38 along the northern shore of Noto Peninsula were obstructed by slope failures and rockfalls near Ozawa village, Saruyama mountain and Kaiso.

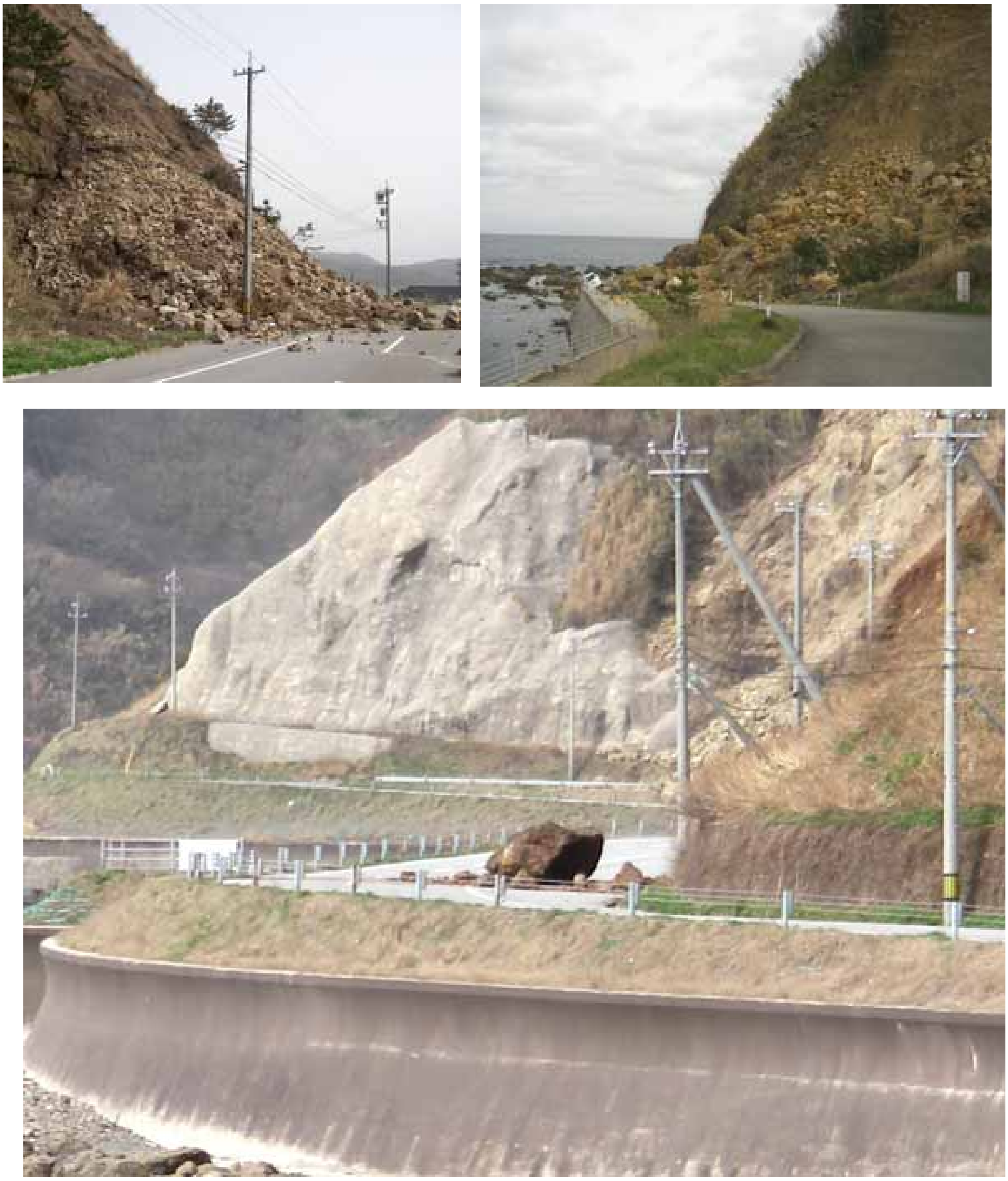

Figure 7.7: Rock slope failures and rock falls obstructing highways

Noto Tollway is closed between Yanagida IC (Hakui) and Tokuta-otsu IC due to extensive embankment failures. The almost entire embankments along this segment of the toll way failed due to ground shaking. The sliding direction of the embankments was eastward. It is considered that the ground shaking together with high ground water pressure could be main causes of the failure of embankments. The authors observed some pools of ground water within the failed part of the embankments nearby at their toes (Figure 7.8).

Figure 7.8: Failure of embankments of Noto Tollway

7.2.3 Tunnels

Since the area is quite hilly and it is well-known sites of landslides, many tunnels were constructed in association with highways, tollways and railway lines. None of tunnels was damaged even they were located next to extensive slope failures (Figure 7.9)

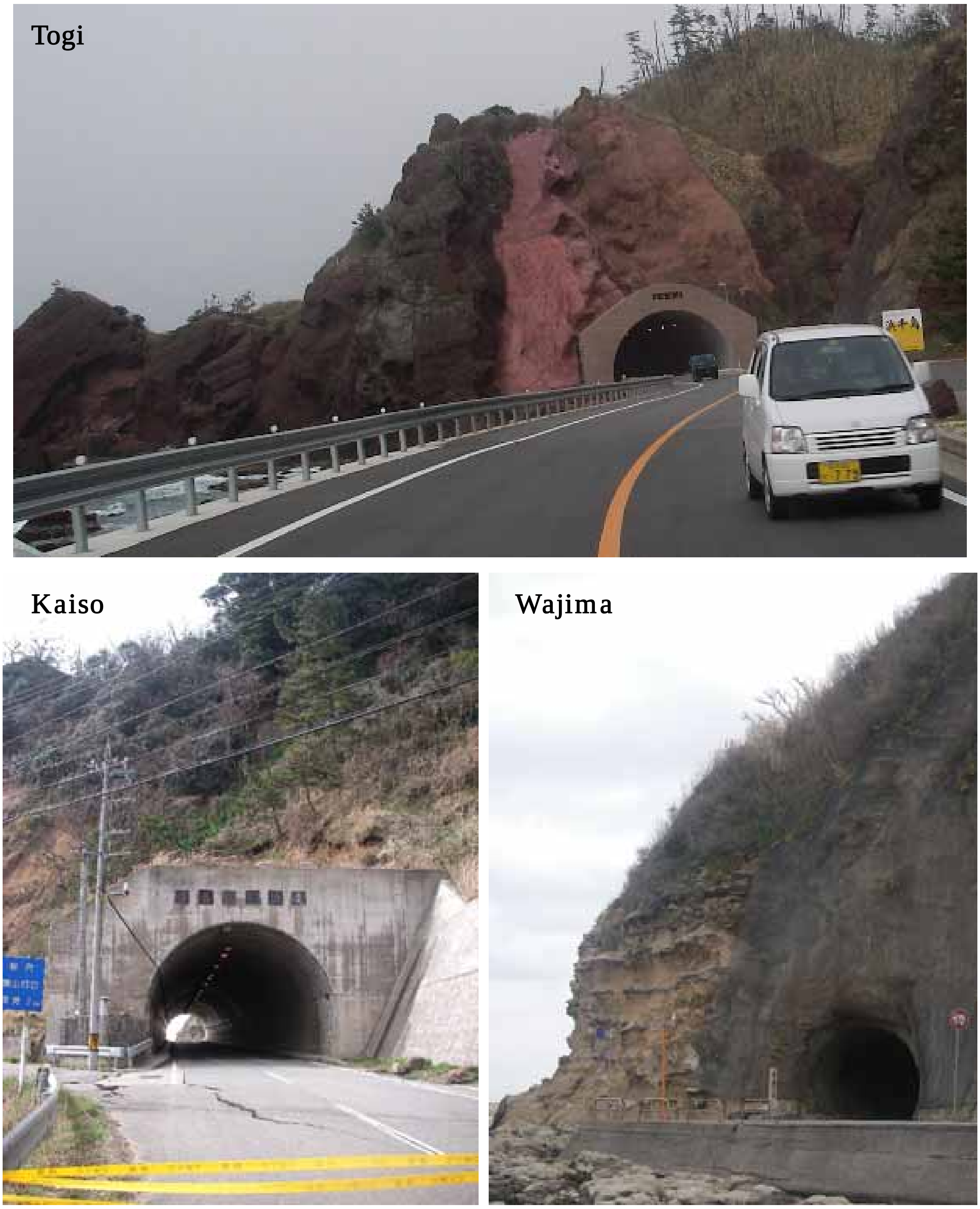

Figure 7.9: Non-damaged tunnels

7.2.4 Bridges and Viaducts

There are several railway and roadway bridges spanning over small rivers, sea and valleys. The long span bridges are Noto viaduct on Noto Tollway, Notojima bridge and Twin bridge connecting Notojima to mainland and Toge viaduct nearby Monzen. Notojima bridge was in the process of retrofitting when the earthquake occurred. Another interesting example of retrofitted viaduct of R1 highway was observed nearby Ichinosaka village. There was no bridge or viaduct collapse in-spite of high ground accelerations. The bridges are generally designed as redundant prestressed structures. Therefore none of girders of the bridges was fallen or damaged during this earthquake. Brief descriptions of the effects of the earthquake on these bridges are described.

(a) Noto Viaduct (bridge)

Noto bridge (viaduct) consists of 4 piers and prestressed curved girders are connected to each other at the mid. It is 400m long and 9.5m wide and it was completed in 1983 (Figure 7.10). The southern embankment of the viaduct was separated from the pier by more than 150mm and it had several open fractures. Furthermore, there were ruptured fragments on the western side of the girders at the middle of the viaduct (Figure 7.11). Although the separation was about 10mm, it seems that the girders might had been collided with each other during the earthquake shaking. The observations from the ground indicated that the eastern side of the connection part is much wider than that on the western side.

Figure 7.10: Views of Noto Viaduct of Noto Tollway

(a) Fractures and embankment separation (b) fragmentation at the connection joint

Figure 7.11: Some examples of damage at Noto Viaduct

(b) Toge Viaduct

Toge viaduct is just south of Toge district of Monzen town. The viaduct consists of 5 piers with a height ranging between 10-13m and separated from each other by a distance of 33m and it has a continuous prestressed girder (Figure 7.12). The girder sits on rubber bearings and It was completed in 1999. The close inspection of this viaduct indicated that the girder was displaced by about 10mm southwardly with a slight rotation. Although none of piers were damaged by ground shaking, one of the rubber bearings at the northern abutment was ruptured as seen in Figure 7.13. The rubber bearings were subjected shearing at both abutments.

Figure 7.12: A view of Toge viaduct (view from south to north)

(a) Ruptured rubber bearing (north side) (b) strained rubber bearing (south side)

Figure 7.13: Views of ruptured and strained rubber bearings

(c) Ichinosaka Viaduct

Ichinosaka is a four-span simple-beam type viaduct (Figure 7.14). The piers are of T-type and they were retrofitted with steel plates. Although there was no visible damage to bearings of the girders, the upper part of the piers underwent some cracking and spalling initiating from the junction between the steel-plates and upper concrete slab (Figure 7.15).

Figure 7.14: A view of Ichinosaka viaduct

Figure 7.15: Piers with spalling

(d) Notojima Bridge

Notojima bridge was completed in 1982 and it is 1050m long. The central part of the bridge is 24.24m high to allow the passage of ships and designed as redundant 3-span box girders. The sides of the bridge consist of simple-structure girders on T-type piers. The bridge was undergoing retrofitting at the time of the earthquake. The earthquake did not cause any damage to superstructure except some embankment and slope failures nearby the abutments.

Figure 7.16: View of Notojima Bridge

(e) Twin Bridge

Twin Bridge was completed in 1999 and it is a 620m long cable-stayed bridge. The center span is 230m long with a clearance of 19m for ship passage. Although there was no visible damage to the superstructure, the embankments at both sides of the bridge were damaged by ground shaking (Figure 7.17). Furthermore, there were some relative settlements between bridge deck and road at embankments. .

Figure 7.17: Views of the bridge and its embankment

(f) Wajima Truss Bridge (Iroha Bridge)

The construction of Iroha Bridge on Kawaharata river was completed in 1962 and it is a single span 50m long simply supported truss bridge (Figure 7.18). The abutment piers of the bridge were recently retrofitted. Cracking occurred at the southern side of the both piers and bearings were deformed at the west abutment due to sliding and rotation (Figure 7.19).

East side West side

Figure 7.18: Iroha truss bridge(view from north to south)

(a) East pier (south side) (b) West pier (south side)

Figure 7.19: Damage at piers and bearings of Iroha Bridge in Wajima City

7.2.5 Noto Airport

The construction of the new Noto airport was completed in 2003 and its runway is 2000m long. The airport was built on a hilly terrain and its construction involved slope cuts and filling of valleys. The construction of Noto Airport was carried out at a quick pace. The large-scale embankment involving a total volume of 16,000,000 m^3 soil and a maximum embankment height of 55m was completed within 3 years (Nagahara et al. 2004). One of the typical cross section of Noto Airport is shown in Figure 7.20 and a grain size distribution of the embankment materials is shown in Figure 7.21. In order to stabilize the soft cohesive soil with high natural water content (wn=30-80%) that was used as the fill material, the embankment was constructed with the use of horizontal geotextile drains to accelerate the consolidation of the compacted wet soil. the drains embedded at 5-m intervals vertically and 2-m intervals horizontally. The earthquake induced some cracks at 22 locations on the runway while the terminal building and control tower were intact except the toppling and sliding of interior items (Figure 7.22). The cracks were quickly repaired and the airport resumed operations on March 26, which was closed on March 25 after the quake.

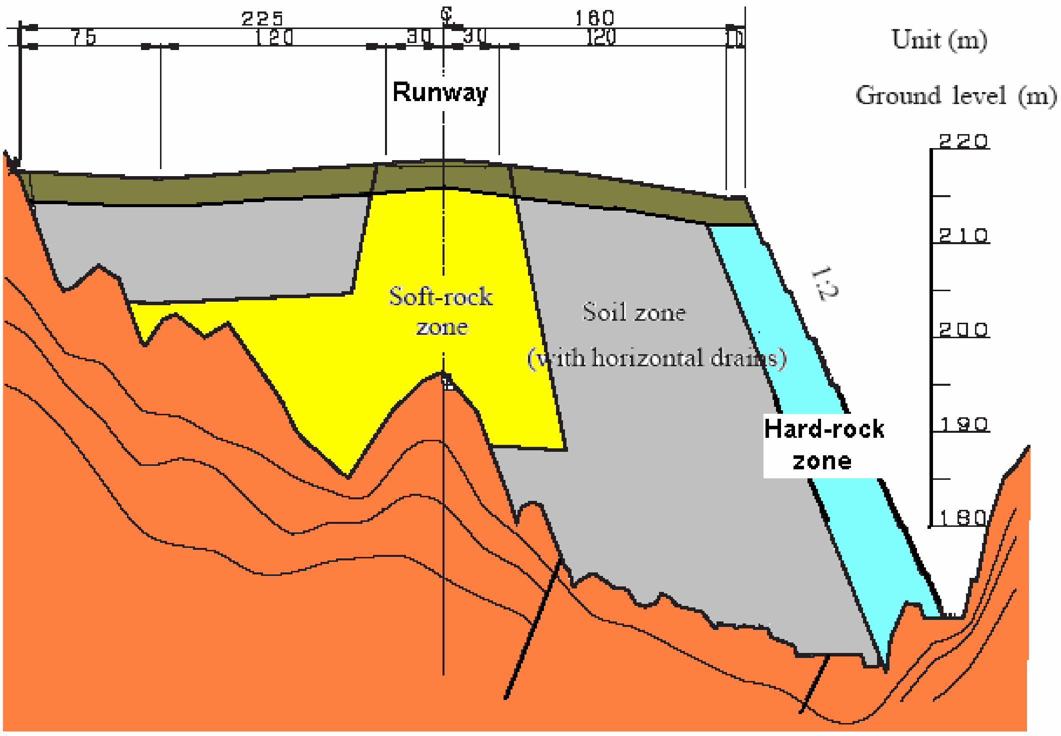

Figure 7.20: A cross section of the highest embankment of Noto airport (from Nagara et al. 2004)

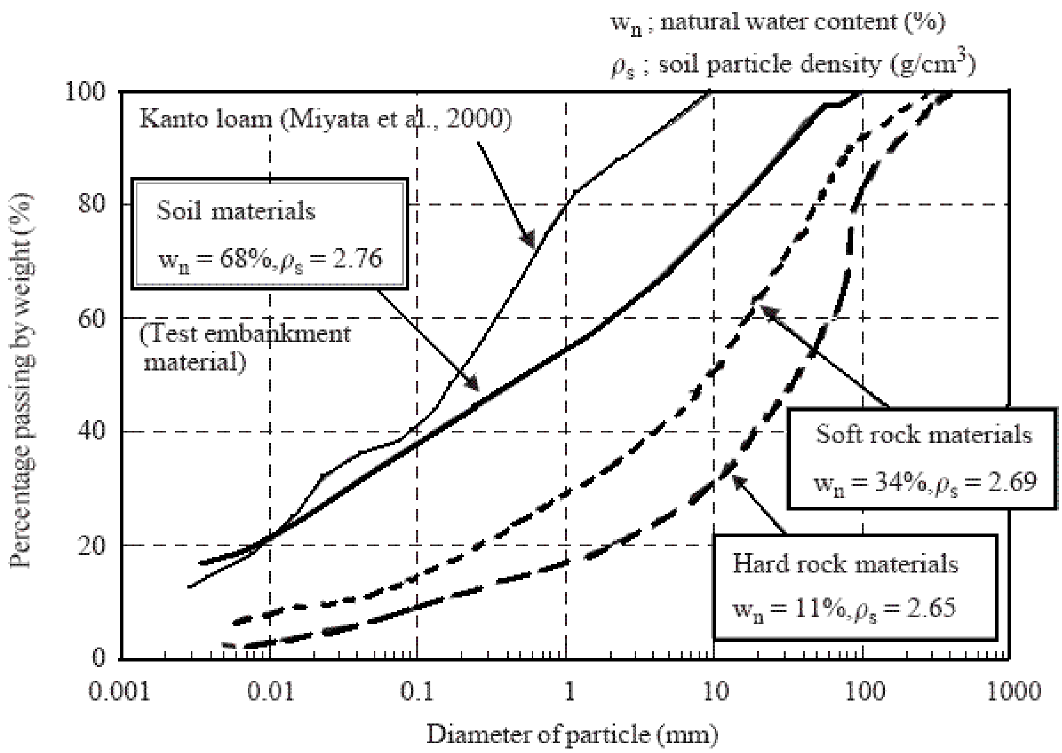

Figure 7.21:Grain-size distribution of embankment of Noto airport (from Nagara et al. 2004)

Figure 7.22: Views of non-damaged control tower and cracked runway at Noto Airport

7.2.6 Ports

The major port facility is located in Nanao City. The second biggest port is in Wajima city. The jetties, piers and quays were partially damaged in the ports of Nanao, Wajima and Kaiso due to ground shaking as well as ground liquefaction. The most extensive damage occurred in Nanao port and the main cause was ground liquefaction. Since the authors visited Nanao port around 19:30 evening, it was difficult to check the overall damage. However, extensive liquefaction and cracking of concrete slabs of quays were observed at many locations (Figure 7.23). Wajima, Shika and Kaiso ports also suffered from the same problem with less severity (Figure 7.24).

(a) ground liquefaction (b) cracking in quay pavement at Ohta district

Figure 7.23: Views of some damage at Nanao port

Figure 7.24: Views of some damage to Wajima port

7.3 Tanks

There is so far no report of damaged storage tanks in the epicentral area. Some storage tanks of petroleum and natural gas are located in major cities in the epicentral area. The authors were only able to inspect petroleum tanks in Wajima and Kaiso ports (Figure 7.25). These tanks are small in size and have a cylindrical shape. The close inspection of the tanks at Wajima and Kaiso ports did not reveal any visible damage.

(a) Tanks at Wajima port

(b) Tanks at Kaiso port

Figure 7.25: Views of tanks at Wajima and Kaiso ports

8 GEOTECHNICAL DAMAGE

8.1 Soil Liquefaction and Lateral spreading

Soil liquefaction was observed at several locations. The authors found traces of liquefaction in the upper and lower parts of Toge district, where the damage was the severest. The liquefaction of ground also occurred in Wajima port area, where the expansion of the port is now implemented. It was very interesting to note that the soil boils observed in a sports ground covered with clayey embankment material while no sand boils were observed along the shore where sand was exposed. The authors consider that the sandy ground should had been also liquefied. The main reason for sand boils might be such that the embankment material acts as an impermeable lid on the liquefied ground and result in prolongation of liquefaction state while ground without such a lid quickly dissipates the excess pore pressure. Since the embankment layer ruptures during shaking, the ruptures acts as vents for sand to come out the surface due to excess pore pressure.

Liquefaction was observed at other locations such as Anamizu, Tatsuruhama and Shika towns, Nanao city of Ishikawa prefecture and Himi town of Toyoma Prefecture. Compared to the effects of ground liquefaction observed during Chuetsu-Niigata earthquake, this earthquake did not cause much damage to structures due to ground liquefaction. The physical and geotechnical properties of one of the soil samples collected are given in Table 8.1 and grain-size distributions are shown in Figure 8.1. Figure 8.2 shows the relation between the hypo-central distance and earthquake magnitude for liquefied sites together with liquefaction state limits. Figure 8.3 shows several views of soil liquefaction in the earthquake-affected area.

Table 8.1: Properties of liquefied soil samples collected from sand volcanoes

Soil Sample Location	Dry Unit Weight (kN/m^3)	Porosity (%)	Mean Grain Size D50 (mm)	Friction Angle (^{o})
Toge-F	14.7	38-4	0.8-1.0	27-30
Toge-SV1	14.9	43.4	0.56	29-32
Toge-SV2	13.4	39.8	0.58	28-31
Wajima	12.6	42.9	0.57	29-32

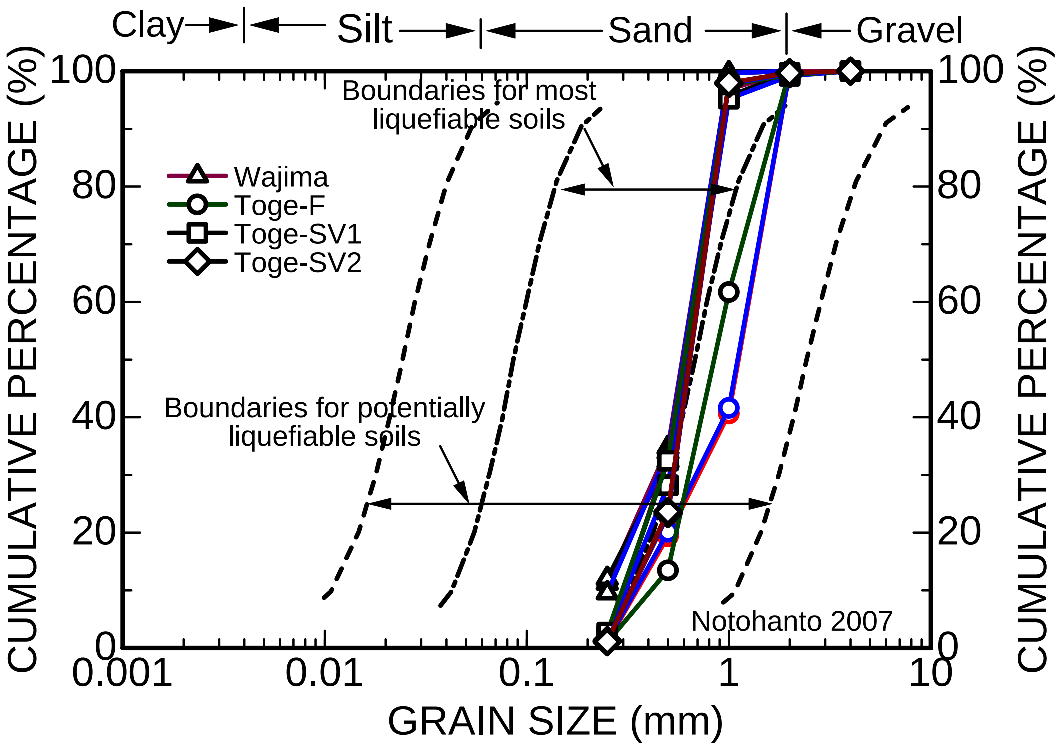

Figure 8.1: Grain-size distribution of liquefied sand

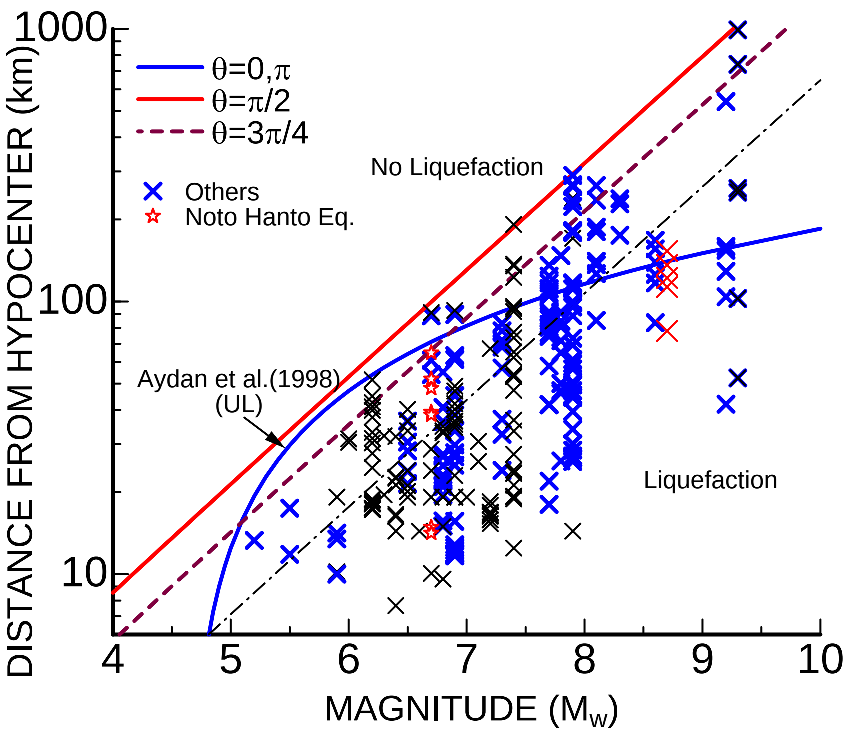

Figure 8.2: The relation between the hypo-central distance and earthquake magnitude for liquefied sites together with liquefaction state limits

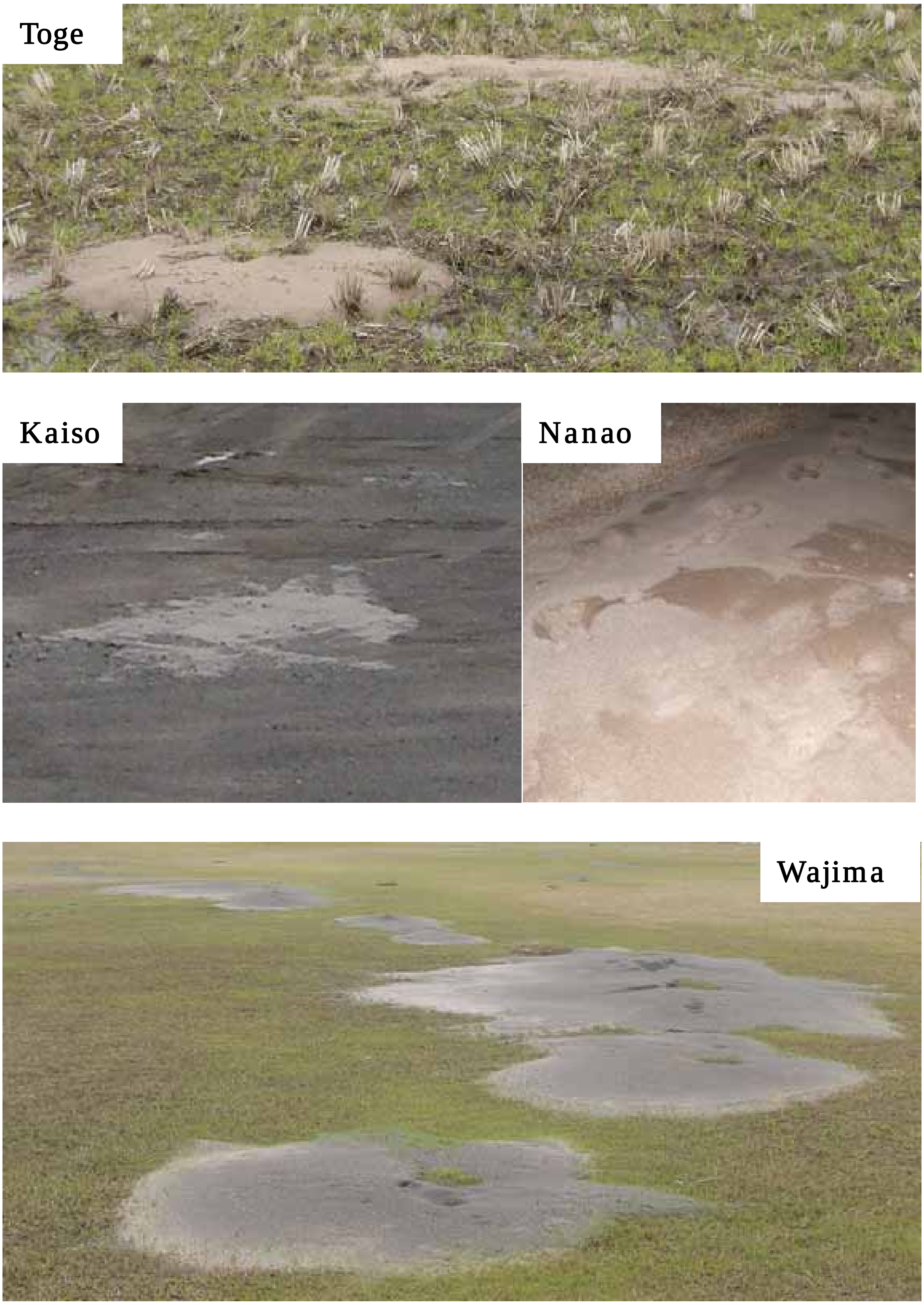

Figure 8.3 Some examples of liquefaction and its effects

8.2 Embankment Failures

Embankment failures and settlements were widespread particularly along Noto Tollway, rivers and creeks. Several typical examples are shown in Figures 7.8, 8.4 and 8.5. The embankments with a height ranging between 20-30m and inclination of 26^{o} were failed. The embankments facing east were failed by ground shaking. The characteristics of embankment material is said to be similar to that used at Noto Airport embankments and it is a soil of volcanic origin. The site investigate indicated that embankment material next to the existing ground was much softer than that at upper parts. Since the existing ground is generally soft volcanic rocks, they constitute an impermeable base. It is likely that the earthquake shaking resulted in excess pore pressure as well as inertia forces to induce the failure of embankments. There were some damage to the embankments of rivers and creeks. However, the height of these embankments was small so that the earthquake did not cause the total collapse of such embankments.

(a) Failed embankment of Noto Tollway

(b) waterpool at the toe of the failed embankment

(a) Embakment failure in Toge district of Monzen town

Figure 8.4: Some examples of embankment failure

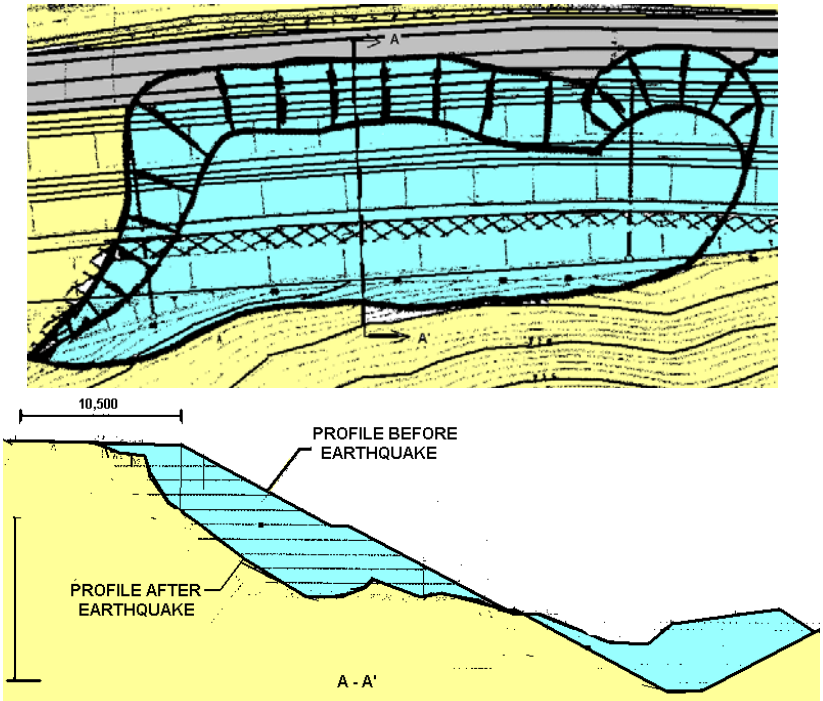

(a) Plan and cross section view of an embankment slide (N37.1584,E136.8565)

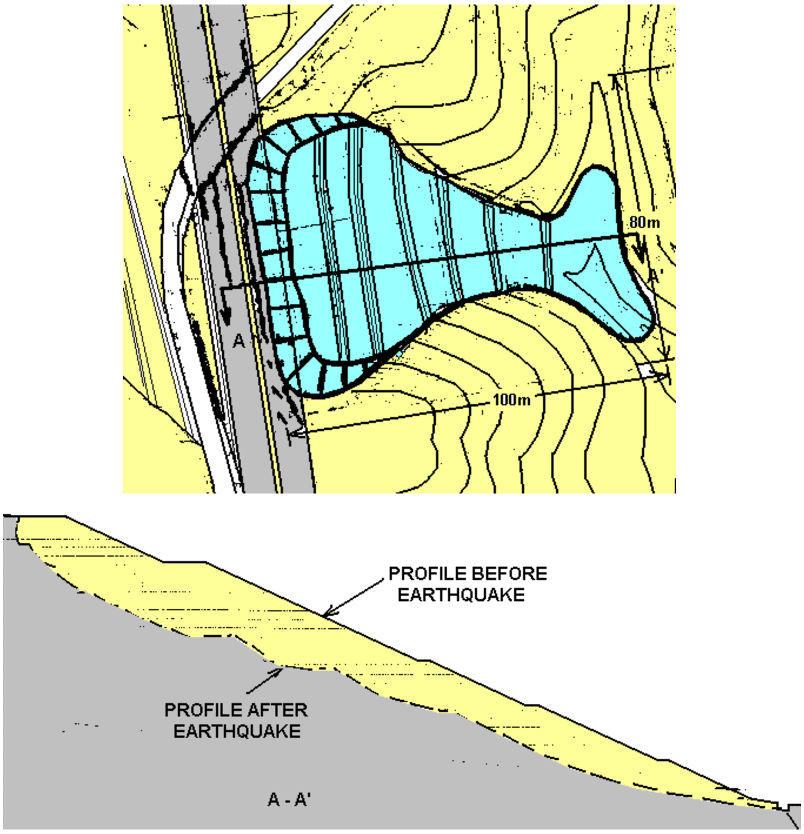

(b) Plane and cross section view of an embankment slide (N37.1745,E136.8577)

Figure 8.5: Plan views of embankment slides at two localities

8.3 Slope Failures

One of the most striking characteristics of this earthquake is extensive slope failures and rock falls in the epicentral area. The slope failures and rockfalls caused extensive damage on roadways, railways and tollways. The most extensive slope failures were observed in Saruyama mountain between Hakka river flowing through Monzen town and northern shore of Noto peninsula. The non-marine volcanic rocks have generally horizontal bedding while marine type volcanic rocks have beddings inclined to NW with an inclination of 20-40 degrees. Furthermore, they have almost vertical open fractures. The thickness of layers change from location to location. Nevertheless, tuff breccia layers are generally thicker than other volcanic and sedimentary rocks. Furthermore, these rocks are subjected to weathering and 1-5m thick weathered zone exists on the slopes. Slopes are generally steep and the inclination is more than 45 degrees along the northern shore of Noto Peninsula.

The authors tried to investigate slope failures in Saruyama mountain. Nevertheless, roadways were obstructed at several locations so that some of slope failures could not be investigated on site. Nevertheless, investigations at several locations of slopes failures clarified the fundamental modes of slope failures. The slope failures may be categorized as

a) Shallow-seated surficial slope failures of weathered rock (Figure 8.6)

b) Combined sliding and toppling failure (Figures 7.7 and 8.7)

d) Rock-falls (toppling, bending failure) (Figures 7.7 and 8.8)

Figure 8.6: Surficial slope failures

Figure 8.7: Combined sliding and toppling failure of rock slopes

Figure 8.8: Toppling failure (from Yomiuri newspaper)

9 DAMAGE TO LIFELINES

9.1 Electricity

The electric supply to the earthquake stricken area was shutdown following the earthquake. Except heavily damaged areas, the electricity was restored on the same day following the earthquake. Hokuriku Electric Power Company provides the electricity supply of the area. In the epicentral region, the power company has a thermal power plant and a nuclear power plant. The units of the power plants were automatically shot-down after the earthquake. Ohta thermal power plant of Hokuriku Electric Power Company was re-activated on March 27. Since problems were observed with pumps for cooling water, the plant operation was suspended until April 1. The thermal plant is in full operation now. The nuclear power plant was not operating during the earthquake due to maintenance work. However, the earthquake caused some spill of radioactive water in the plant.

Figure 9.1: A view of Ohta Thermal power Plant in Nanao City

The electricity distribution system in the region is done through poles and high- voltage transmission lines. Although concrete poles were inclined as a result of partial bearing failure of the surrounding ground, none of transmission towers were damaged or toppled during this earthquake (Figure 9.2). The poles having transformers mounted on were particularly suffered more and also the poles were inclined in heavily liquefied areas. Nevertheless, the repair works on electricity distribution system could be accomplished in a short period of time. The main transmission lines are elevated and supported through 40-50m high steel pylons. In-spite of wide spread slope failures, there was no damage to pylons. Since the power was provided from other power plants of the electricity network and electricity distribution system was intact, the recovery of electricity was quite rapid.

Figure 9.2: Inclined or damaged poles in Monzen town

9.2 Water Network

The water networks were particularly damaged in Monzen town and Wajima City. Initially 13000 households were out of water. The damage to water network is generally associated with pipe breakage at joints. The water distribution system was fully restored on April 7.

9.3 Natural Gas Network

The natural gas system is only used in Nanao City, which is about 51km away from the earthquake epicenter. Most of households utilize propane gas in the epicentral area. No fire associated with propane gas etc. was reported .

9.4 Sewage System

The sewage systems were damaged by the liquefaction and/or settlement of back- fill soil (Figure 9.3). The uplift of manholes could be observed in Monzen town. The uplift of manholes was as much as 600mm.. The local authorities now have been checking the sewage system and replacing the sections underwent uplifting or rupturing. Since the permanent ground deformations occurred due to lateral spreading of ground as a result of liquefaction, the joints of the sewage system suffer some leakage and need repairs.

(a) Motoichi-Monzen (b) Wajima

Figure 9.3: Settlement of backfill material of sewage systems and their repair

9.5 Telecommunications

Telecommunication system suffered the same problem due to heavy telecommunication traffic as observed in other earthquakes and there was no incidence of damage or toppling of relaying towers. Besides the conventional telephone system, the mobile telephone systems of Docomo, Softbank and AU are used widespread. Particularly Docomo system suffered from heavy telecommunication traffic following the earthquake. However, the systems become normal next day.

10 CONCLUSIONS

2007 Noto Peninsula earthquake caused widespread damage particularly in the epicentral area. The main characteristics of this earthquake can be summarized as follows:

1) The faulting was of thrust type and it was an off-shore intra-plate earthquake. However, some surface ground ruptures were observed at several places, which may be associated with secondary faulting.
2) Very large aftershocks have been observed and they are still continuing. It seems that the faulting plane propagated in NE direction towards Wajima city.
3) High ground accelerations with pronounced directivity effects did occur although the magnitude of earthquake is relatively small compared with, for example, 1995 Kobe earthquake. Due to close proximity of the epicenter, the shaking effects become more pronounced.
4) Permanent deformation of ground associated with faulting did occur although no distinct ground ruptures observed. In addition to the effects of the faulting, the ground liquefaction may have contributed to the heavy damage in Toge district of Monzen town.
5) Ground liquefaction was observed throughout the epicentral region. The liquefaction caused lateral spreading and damage on some linear structures and port facilities through relative movements, uplifting or settlement.
6) Many rock and soil slope and embankment failures took place, particularly in the mountainous area and along rivers. These slope and embankment failures destroyed roadways and Noto Tollway. The large scale rock slope failures were directly associated with structural discontinuities in rock mass such as existing faults, bedding planes and vertical joints.
7) The permanent ground deformations as well as ground shaking caused some structural damage to residential houses, buildings, bridges, roads, highways, railways, tollways and lifelines.

REFERENCES

Aydan, Ö., Y. Shimizu, Y. Ichikawa (1989). The Effective Failure Modes and Stability of Slopes in Rock Mass with Two Discontinuity Sets. *Rock Mechanics and Rock Engineering*, **22**(3), 163-188.

ERI (2007): http://www.eri.u-tokyo.ac.jp/topics/

Ito,K., Wada, H., Watanabe, K., Horikawa, H., Tsukuda, T. and Sakai, K. (1994): 1993 Off Noto Peninsula Earthquake, Annuals, Disas. Prev. Res. Inst., Kyoto Univ., No.37, B-1, 325-341.

GSJ(2007): http://www.gsi.go.jp/BOUSAI/ (in Japanese)

HARVARD:Source process. http://www.globalcmt.org/cgi-bin/globalcmt-cgi-bin/

JMA(2007): http://www.seisvol.kishou.go.jp/eq/ (in Japanese)

K-net (2007): http://www.k-net.bosai.go.jp/

KiK-Net (2007): http://www.kik.bosai.go.jp/

Lopez, J.C. and Ishiwatari, A. (2002): Petrogenesis of the tholeiitic basalt, calc-alkaline basaltic andesite and high magnesian andesite lava succession of the Oligo-Miocene Anamizu Formation in northeastern Noto Peninsula, Central Japan. J. Mineralogical and Petrological Sciences, Vol. 97, 85-113.

Nagahara, H., Fujiyama,T., Ishiguro, T., Ohta, H. (2004): FEM analysis of high airport embankment with horizontal drains. Geotextiles and Geomembranes 22, 49-62.

NIED(2007): http://www.hinet.bosai.go.jp/topics/

USGS (2007): http://earthquake.usgs.gov/

Yahoo Japan (2007): http://dailynews.yahoo.co.jp/

Yagi, Y. (2007): Source process of Noto peninsula earthquake (in Japanese) http://www.geo.tsukuba.ac.jp/press_HP/yagi/EQ/20070325/

Yomiuri Newspaper (2007): http://www.yomiuri.co.jp/